Raman fiber lasers



2017 J. Opt. 19 023001

(http://iopscience.iop.org/2040-8986/19/2/023001)

**IOP** Publishing Journal of Optics
J. Opt. **19** (2017) 023001 (26pp) doi:10.1088/2040-8986/19/2/023001

## Topical Review

# Raman fiber lasers

**V R Supradeepa[1], Yan Feng[2] and Jeffrey W Nicholson[3]**

[1] Centre for Nano Science and Engineering, Indian Institute of Science, Bangalore 560012, India
[2] Shanghai Key Laboratory of Solid State Laser and Application, and Shanghai Institute of Optics and Fine Mechanics, Chinese Academy of Sciences, Shanghai 201800, People's Republic of China
[3] OFS Laboratories, 19 Schoolhouse Road, Somerset, New Jersey 08873, USA

E-mail: supradeepa@cense.iisc.ernet.in, feng@siom.ac.cn and jwn@ofsoptics.com

Received 17 August 2015, revised 14 September 2016
Accepted for publication 13 October 2016
Published 4 January 2017

**Abstract**
High-power fiber lasers have seen tremendous development in the last decade, with output powers exceeding multiple kilowatts from a single fiber. Ytterbium has been at the forefront as the primary rare-earth-doped gain medium owing to its inherent material advantages. However, for this reason, the lasers are largely confined to the narrow emission wavelength region of ytterbium. Power scaling at other wavelength regions has lagged significantly, and a large number of applications rely upon the diversity of emission wavelengths. Currently, Raman fiber lasers are the only known wavelength agile, scalable, high-power fiber laser technology that can span the wavelength spectrum. In this review, we address the technology of Raman fiber lasers, specifically focused on the most recent developments. We will also discuss several applications of Raman fiber lasers in laser pumping, frequency conversion, optical communications and biology.

Keywords: Raman scattering, nonlinear optics, fiber lasers, Raman laser, supercontinuum, fiber optics, optical communications

(Some figures may appear in colour only in the online journal)

## 1. Introduction

### 1.1. Technology of high-power fiber lasers

High-power fiber lasers have seen tremendous development in the last decade, with output powers exceeding 10 kW from a single fiber [1]. This development is fueled simultaneously by industrial and defense applications. This rapid advance in technology has occurred with rare-earth-doped fiber lasers, specifically ytterbium-doped fiber lasers, being at the forefront. In these lasers, low-brightness and low-efficacy light from semiconductor laser diode modules is converted to high-brightness, high-efficacy light using double-clad optical fibers with a rare-earth-doped core. Since most laser applications rely on the optical intensity, for a given optical power, high-brightness light from fiber lasers has substantially more utility than the light directly out of laser diodes, which is of low brightness. Ytterbium has several inherent material advantages such as low quantum defect between the absorbed pump light and the emitted signal light and the ability to be doped into fibers at enhanced concentrations while maintaining laser efficiency. The consequence of this is low thermal load and enhanced efficiency, which enables power scaling.

Figure 1 shows the evolution of the output power from fiber lasers over the last two decades (figure from [1]). Except the data point from 20 years ago, all the other results are with ytterbium-doped fiber lasers. Though the power scaling has been prolific, many applications rely upon the diversity of emission wavelength. Several of these applications will be discussed in this review. As will be seen in the next section, owing to the reliance on ytterbium as the primary gain medium, power scaling of fiber lasers so far is largely confined to a narrow emission region (from 1050 to 1120 nm).

### 1.2. Limitations of gain from rare-earth dopants

Figure 2 shows the relative power scaling of different fiber laser technologies today. Each rare-earth-doped fiber laser,

 

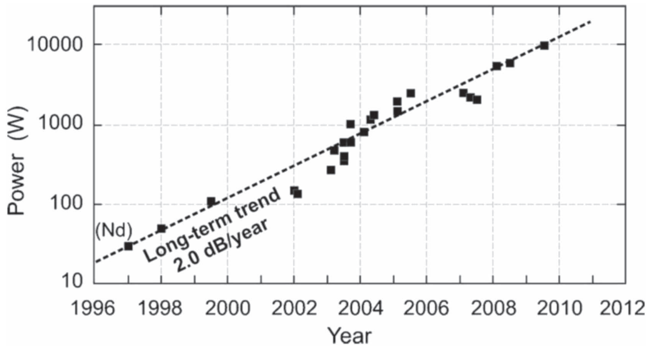


**Figure 1.** Power scaling of fiber lasers (from [1]).

corresponding to the dopant in it, has a specific emission window. The window of emission wavelengths from ytterbium-doped fiber lasers is limited to a small band (1050–1120 nm). In this region, it is now common to have standard fiber laser modules which can emit over 3 kW of power. Other rare-earth-doped fiber lasers such as thulium/holmium (1900–2100 nm) and erbium, erbium–ytterbium (1530–1590 nm) partly complement the emission range. However, they are significantly limited in power and efficiency compared to ytterbium-doped fiber lasers. The thulium lasers have achieved power levels of around a kilowatt [2] and the erbium lasers are limited to a few hundred watts [3]. Higher quantum defect, difficulty in increasing the doping levels to enhance absorption, quenching, ion-pair formation, etc are all reasons which contribute to the other rare-earth dopants not performing as well as ytterbium.

As a result, other than the narrow 1050–1120 nm band, power scaling is largely limited. However, there is a much more significant problem. There are substantial white spaces in the wavelength spectrum where no rare-earth fiber laser technology is available. This is a significant constraint, since several desirable attributes for high-power applications are lacking in the ytterbium emission window but are available at other wavelengths. An example would be eye safety. According to the maximal permissible exposure to the human eye, the 1.5 $\mu$m wavelength is several (three to four) orders of magnitude safer than the 1 $\mu$m region [4]. An important application involving lasers would be free-space propagation. Here again, the 1 $\mu$m region is not the best suited for atmospheric transmission compared to wavelength bands at longer wavelengths [5]. In addition, there are other applications such as pumping other lasers (primarily nonlinearity constrained systems such as pulsed or narrow-linewidth lasers) which need pump lasers which can provide sufficient powers in the white spaces currently [6]. For these reasons, lasers which span the wavelength space while providing high powers in a scalable way need to be developed.

### *1.3. Wavelength agile high-power lasers: Raman fiber lasers*

Currently, Raman fiber lasers (first proposed in [7]) are the only known wavelength agile, high-power fiber laser technology that can span the wavelength spectrum and cover the white spaces. Raman fiber lasers leverage the technology of high-power, rare-earth-doped fiber lasers (such as ytterbium) which serve as their input and convert it to any desired wavelength region using one or more wavelength shifts of stimulated Raman scattering in optical fibers. Figure 3 shows a schematic diagram of this process. A high-power laser in an accessible region creates a series of Raman–Stokes shifts, which can lead to conversion to wavelengths higher than the starting wavelength. The area of Raman fiber lasers has seen extensive development in the last few years on various fronts. Some key technical aspects which are being researched include new laser architectures, scaling output power, improving efficiency, enhancing wavelength diversity and improved spectral quality. In particular, some important goals are to achieve close to quantum-limited conversion efficiency in this conversion and to stop the cascaded Raman conversion at the desired wavelength.

There has also been significant work in novel and niche implementations of Raman lasers. Complementary to the development of Raman fiber lasers themselves, there has also been extensive work on using Raman fiber lasers in various applications ranging from optical pumping and nonlinearity mitigation in fiber lasers to optical communications to biology. In this review, we address the technology of Raman fiber lasers and its applications, specifically focused on the most recent developments.

## 2. Operation of Raman fiber lasers

In this section, we will deal with the physical mechanism enabling Raman fiber lasers and conventional architectures for Raman fiber lasers. In later sections, we will describe newer architectures for Raman fiber lasers and discuss how they improve upon the conventional techniques described here.

### *2.1. Stimulated Raman scattering in optical fibers*

The mechanism for gain in Raman fiber lasers, as the name suggests, is stimulated Raman scattering. Optical fibers offer an excellent medium for utilizing stimulated Raman scattering. Some key performance aspects are

a. low linear loss, which enables long interaction lengths,
b. ability to confine light to small mode areas, which can significantly enhance nonlinearity, and
c. Raman gain in optical fibers spans substantial bandwidth. This is made possible by the inhomogeneous broadening in silica or other glassy materials which constitute the optical fiber.

Figure 4 shows the representative gain spectrum in a silica optical fiber (from [8]). The spectrum shown is for the case of a germanosilicate fiber, and in later sections we will be dealing with other types of optical fiber. For the germanosilicate fiber, which is the most common variety, and includes fibers used in transmission and fiber laser applications, the peak Raman gain occurs at an offset of 13.2 THz below the pump frequency. However, as shown in the gain spectrum,

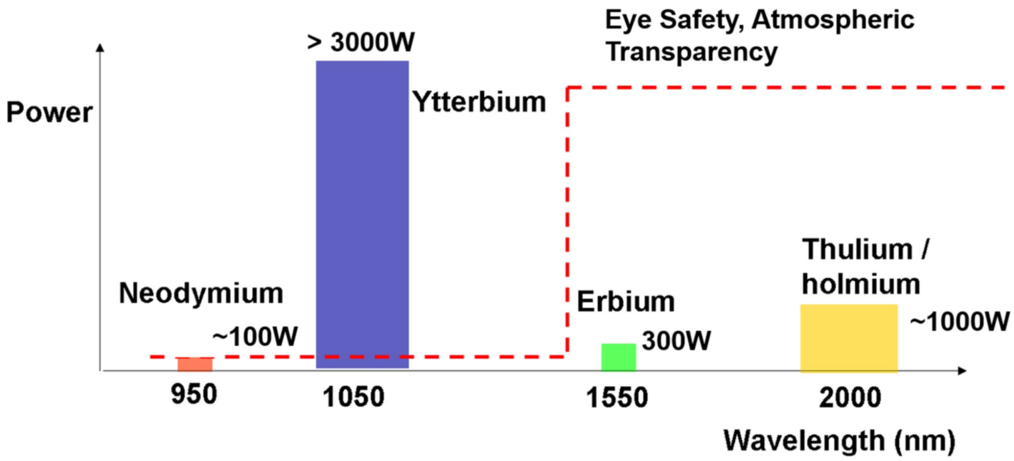


**Figure 2.** Various rare-earth-doped, high-power fiber laser technologies.

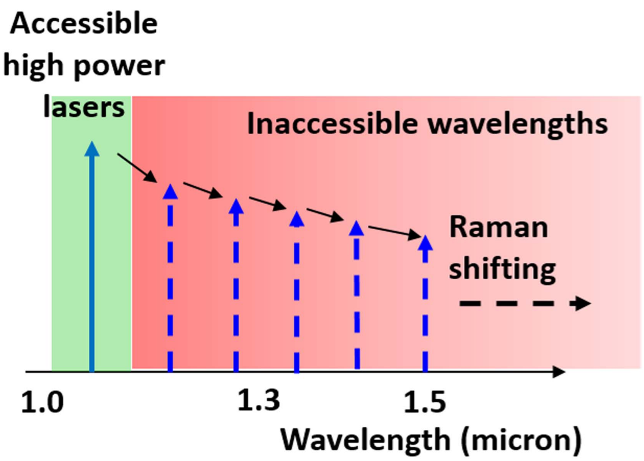


**Figure 3.** Schematic diagram of cascaded Raman conversion.

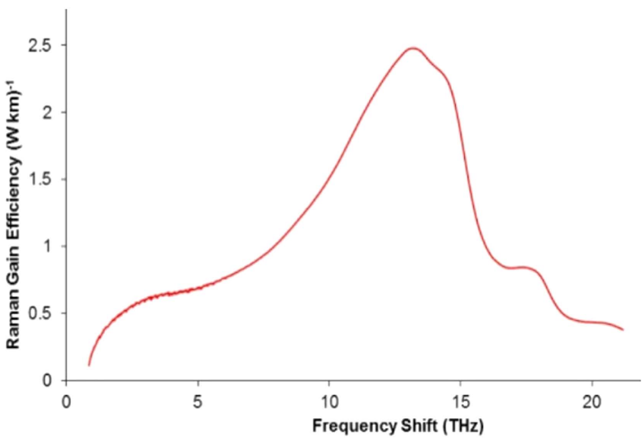


**Figure 4.** Representative Raman gain spectrum in a silica optical fiber (from [8]).

there is substantial gain at offset frequencies well beyond the peak gain.

### 2.2. Common implementations of Raman fiber lasers

Raman lasers can be broadly classified into two general categories. In the first case the wavelength is shifted by one

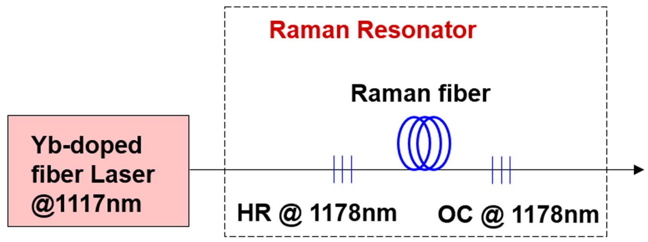


**Figure 5.** Schematic diagram of a Raman fiber laser with one wavelength shift (HR—high-reflectivity fiber Bragg grating, OC—output coupler—a low-reflectivity fiber Bragg grating).

Raman–Stokes shift, and in the second case the wavelength is shifted by multiple Raman–Stokes shifts. The latter is called a cascaded Raman laser.

*2.2.1. Single wavelength shift.* In Raman lasers with a single wavelength shift, a high-power rare-earth-doped fiber laser (commonly ytterbium) is connected to a Raman resonator, which involves a resonant cavity at the next Stokes wavelength. In some implementations, a pump reflector is used on the output side to enhance the interaction between the pump and the Raman-shifted signal [7, 9]. To provide directionality to the laser emission, a high-reflecting fiber Bragg grating (reflectivity $> 99\%$) is used on the input side and the output side is a low-reflectivity output coupler. The reflectivity of the output coupler depends on the power level of the Raman laser. However, at the few watt level, it is common to have output reflectivity $< 10\%$. A long length of fiber is spliced between the two gratings. Key attributes of the fiber include high Raman gain and long interaction lengths. Further, dispersion aspects of the fiber are important to ensure that the primary nonlinearity being utilized is stimulated Raman scattering. The fibers used for this purpose will be discussed in more detail in the next section.

Figure 5 shows a schematic diagram of a specific Raman fiber laser with one wavelength shift. In this particular case, the laser uses a 1117 nm ytterbium-doped fiber laser and converts it to 1178 nm. Frequency-doubled 1178 nm lasers emitting in the yellow at 589 nm have found use in various applications including as laser guide stars. This will be

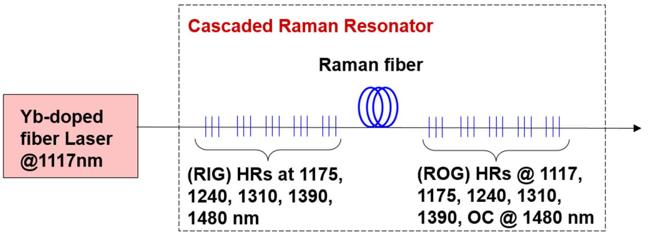


**Figure 6.** Schematic diagram of a cascaded Raman fiber laser with multiple wavelength shifts (RIG—Raman input grating set, ROG—Raman output grating set).

described in later sections on applications. The resonator which converts 1117 nm to 1178 nm has HR and OC gratings at 1178 nm. Not shown is a pump reflector HR grating on the OC side at the 1117 nm wavelength. In this particular case, the frequency difference between 1117 nm and 1178 nm is close to the frequency offset for peak Raman gain.

*2.2.2. Multiple wavelength shifts: cascaded Raman resonator.* Wavelength conversion over two or more Stokes shifts is performed through the use of a cascaded Raman resonator (as shown schematically in figure 6). It is comprised of nested cavities at each of the intermediate wavelengths made with fiber Bragg gratings (referred to as the Raman input and output grating sets) and a low-effective-area (high-nonlinearity) fiber (Raman fiber). Each intermediate wavelength in the resonator is chosen to be close to the peak of the Raman gain of the wavelength preceding it. A low-reflectivity output coupler terminates the wavelength conversion. At the output, most of the light is at the desired final wavelength with small fractions at the intermediate wavelengths.

In the case shown in figure 6, the laser again uses a 1117 nm ytterbium-doped fiber laser and converts it to an output at 1480 nm. High-power 1480 nm lasers have found extensive use as pump sources for core pumping of erbium-doped fiber amplifiers. This will be described in later sections on applications. Further, as described in the introduction, by achieving the conversion close to the 1.5 $\mu$m band as in this case, the laser becomes substantially eye safe and its attractiveness for a variety of laser applications involving human operators is enhanced.

## 3. Systems and components

In this section, we will look briefly into the key components and systems forming a Raman fiber laser. The primary constituents are a high-power fiber laser source, fiber Bragg gratings and a long length of optical fiber. Each of the components are in use in some form in conventional fiber lasers. In addition, at higher powers, some additional components for isolation between the rare-earth-doped fiber laser and the cascaded Raman resonator are necessary to enhance isolation. This aspect will be covered in the last part of this section.

### *3.1. High-power rare-earth-doped fiber lasers*

In recent years, cladding-pumped fiber lasers and amplifiers have emerged as the technology of choice for obtaining high powers. Figure 7 shows a schematic diagram of a cladding-pumped fiber amplifier. A double-clad fiber with a rare-earth-doped core (ytterbium for most industrial applications) is used. The core is single moded or few moded. An inner cladding in the fiber, which helps guide light in the core, is itself a highly multi-moded light guide for the pump light (shown in figure 7). Low-brightness pump light (in the 900–980 nm region for ytterbium) is coupled into the inner cladding of the fiber and a signal (usually in the 1050–1120 nm region for ytterbium) is coupled into the core. The cladding light absorbed by the doped core is re-emitted into the core as a high-brightness beam. A rare-earth-doped fiber laser is primarily a brightness converter from the low-brightness pump diodes to high-brightness signal output.

Figure 8 shows a schematic diagram of a standard, rare-earth-doped, cladding-pumped fiber laser. The mechanism for gain is the cladding-pumped amplifier and two gratings at the end provide the necessary feedback. Multiple diode modules are power combined using a fiber pump combiner, which is then spliced to the laser resonator. Extensive details on the design and analysis of these lasers are now available [1].

### *3.2. Raman wavelength conversion*

Raman wavelength conversion primarily involves three key components—optical fibers for providing Raman gain, fiber Bragg gratings for feedback and components for isolation between the rare-earth-doped fiber laser and the Raman converter.

*3.2.1. Optical fibers for Raman conversion.* Long lengths of optical fibers are used to provide the necessary Raman gain for wavelength conversion. The following are some important parameters that characterize the fiber.

- *Effective area.* Raman gain is enhanced with increasing optical intensity. This is equivalent to Raman gain being higher in fibers with smaller effective area. For this reason, fibers used for Raman lasers tend to have small effective areas. Fibers used in Raman fiber lasers have an effective area between 10 and 15 $\mu m^2$ at 1100 nm. In order to maintain the effective area with the same level of guiding, the refractive index of the core is further enhanced. This is usually achieved in silica fibers through greater germanium doping.
- *Dispersion.* It is well known that a laser with sufficient power propagating in a fiber in the anomalous dispersion regime generates a supercontinuum [10]. Even in the normal dispersion regime, reduction in dispersion results in more efficient line broadening by four-wave mixing [11]. Both these effects are counter-productive to the cascaded Raman conversion, since they results in substantial reduction in spectral brightness. Optical fibers used in Raman lasers thus need to have a large dispersion coefficient. Conventional Raman fibers [8] have a

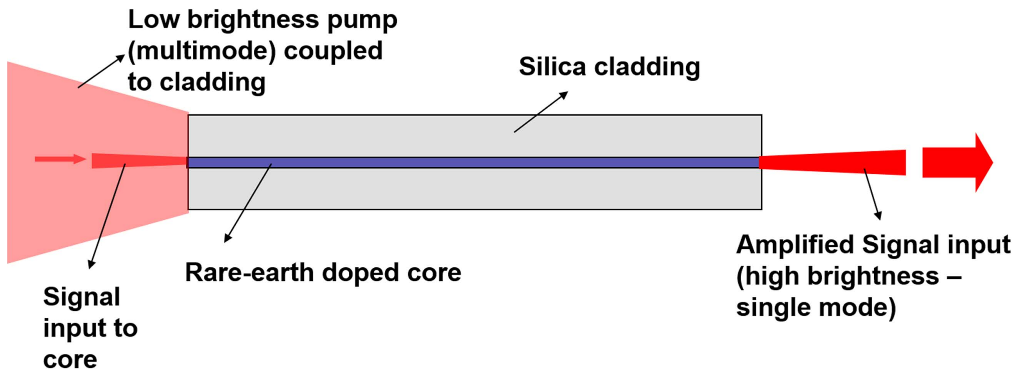


**Figure 7.** Schematic diagram of the operation of a rare-earth-doped, double-clad fiber amplifier. The first cladding enables the guiding of light in the core and acts as the light guide for the pump light.

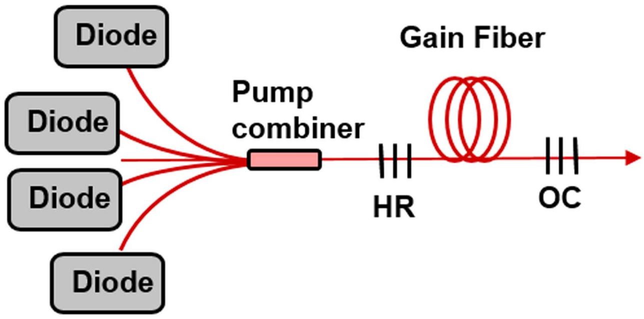


**Figure 8.** Schematic diagram of a cladding-pumped, rare-earth-doped fiber amplifier.

dispersion coefficient as high as $-80\ \text{ps nm}^{-1}\ \text{km}^{-1}$ in the wavelength region of interest. Coincidentally, reduction in effective areas (by the use of smaller cores) also results in enhancement of dispersion. This is another positive offshoot of using smaller-effective-area fibers for Raman lasers.

- *Loss.* The loss in a fiber is an important factor deciding the efficiency of Raman conversion. Typically, fibers used in Raman lasers have the same loss as standard single-mode fibers. $1/(\text{loss} \times \text{effective area})$ can be used as an informal figure of merit, and owing to similar loss numbers but much smaller effective area the figure of merit for Raman fibers is much higher compared to conventional single-mode fibers. An important aspect, however, is that different fibers have different low-loss wavelength windows. For example, the silica fiber, which is used in a majority of optical fiber applications, is very lossy in the mid-IR region and thus cannot be used for mid-IR Raman lasers. Currently, Raman lasers operate in two main wavelength bands. In the near-IR region, silica fibers are primarily used. In the mid-IR region, fluoride or chalcogenide fibers are used [12, 13]. In this work, unless explicitly mentioned, the fibers are silica fibers. We will briefly look into the other fibers in the context of mid-IR Raman lasers in a later section.
- *Frequency shift.* The peak Raman gain in a specific fiber can be different based upon the material composition. Conventional fibers based on silica have a frequency shift of 13.2 THz as shown in figure 4. However, alternate fibers exist which have different Raman shifts. An important alternative is the phosphosilicate fiber, which has a peak gain at ~40 THz. Having a larger Raman shift is a desirable attribute for many applications since this necessitates fewer Stokes shifts to reach the final desired wavelength. Figure 9 shows a comparison between the Raman gain spectrum in silica fibers and phosphosilicate fibers. An important point to note is that, though the peak gain might be at a specific frequency shift, at high enough powers there can be lasing at all frequencies with sufficient Raman gain. For this reason, phosphosilicate-fiber-based lasers have not been used at higher powers, since simultaneous lasing at both the silica lines as well as the phosphosilicate lines is seen.

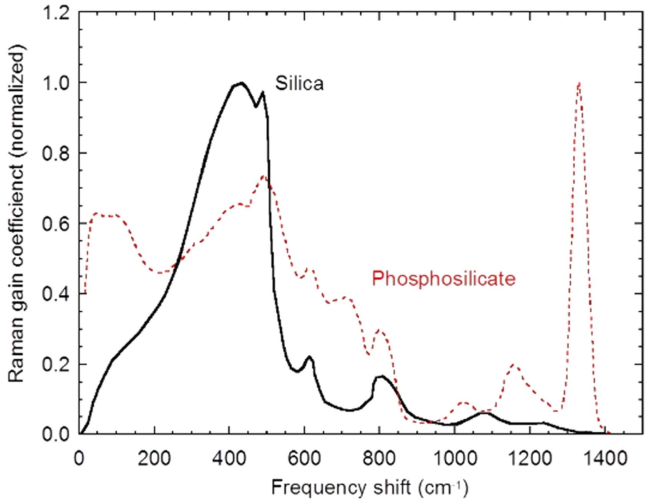


**Figure 9.** Comparison of Raman gain coefficient in phosphosilicate fibers and silica fibers (from [14]).

*3.2.2. Fiber Bragg gratings for the Raman resonator.* Fiber Bragg gratings are key components of the Raman resonator and their fabrication is similar to the fabrication of other fiber Bragg gratings [15]. However, the following points need to be noted, which are specifically important for Raman resonators.

- *Grating fibers.* Conventionally, fiber Bragg gratings for fiber lasers are fabricated on standard fibers. However, in this case, since the splice loss between standard fibers and the specialty Raman fibers can be high, it is desirable to have the gratings for the Raman resonator on the same fiber as used for gain. This approach minimizes the splice loss.

- *Gratings in sets.* Depending on the number of Stokes shifts in the cascade, several gratings would have to be spliced at the input and the output of the Raman resonator to make the nested cavities. If each grating were to be fabricated independently, this would result in substantial efficiency reduction due to multiple splices. For this reason, all the Bragg gratings needed for the Raman resonator on one side are fabricated on a single length of fiber. The input side (all high reflectors) is known as the Raman input grating set (RIG) and the output side is known as the Raman output grating set (ROG). To further minimize losses, the RIG and ROG can be fabricated directly on the Raman fiber, making it a monolithic entity without the need for any splices.
- *Power handling.* The gratings in the Raman resonator are highly reflecting and handle very high power levels (tens of watts). For this reason, it is essential for the process of grating fabrication to be refined in order to handle the power levels. Fiber fusing [16] is a common issue which can occur if the gratings cannot handle the power, and this can be very deleterious.

*3.2.3. Components for isolation.* In its simplest form, a cascaded Raman fiber laser consists of a rare-earth-doped fiber laser cavity followed by a Raman resonator cavity. Thus there is a risk of the cavities coupling together, causing instabilities due to feedback. In practice, however, when operating a cascaded Raman at modest power levels of up to a few tens of watts, the lasers operate stably without any effort at isolation between the rare-earth cavity and the Raman cavity [17, 18]. Even at 40 W output power, a 1480 nm Raman laser could operate stably without isolation between the cavities [19].

At higher operating powers, however, the stability of the system can suffer substantially due to feedback [20, 21]. The rare-earth-doped cavity is followed by the first high reflector in the Raman cavity, which is designed to be a high reflector at a wavelength that is one Stokes shift away from the operating wavelength of the rare-earth cavity. This Stokes reflectivity then leads to backward Stokes lasing in the rare-earth cavity, initially causing temporal fluctuations at the onset of Stokes lasing [21], and ultimately ending in laser failure if the system is pushed further.

Therefore, for stable high-power operation of Raman fiber lasers, the rare-earth fiber laser cavity should be isolated from the backward propagating Stokes wavelength. In principle, a fiber-coupled optical isolator could perform this function. Unfortunately, to date, power handling of fiber-coupled isolators significantly lags the power generation capacity of fiber lasers. The maximum power handling of commercially available, fiber-coupled isolators is currently around 50 W, but more than 1 kW of 1 $\mu$m radiation from an ytterbium fiber laser has been used to pump fiber Raman lasers.

Fortunately, the backward propagating lasing of the Raman cavity grating is Stokes shifted, so a frequency selective element can be used to isolate the rare-earth laser cavity from the Raman laser cavity. Perhaps the most effective element for isolating the cavities is a fused-fiber wavelength division multiplexer (WDM). Fused biconical tapers [22, 23] can provide wavelength selective directional couplers with very low loss, an important characteristic for high-power fiber laser operation. Single-mode WDMs provide low-loss throughput for the high-power rare-earth laser output to the Raman laser cavities, while diverting the backward propagating Stokes-shifted light away from the rare-earth cavity. These WDMs have been demonstrated to isolate the rare-earth cavity from the backward Stokes lasing to provide stable operation [20], and have been successfully operated with more than 400 W of input power [24].

Another option for wavelength selective isolation of the backward Stokes is UV inscribed gratings. A long-period grating (LPG) provides phase matching between modes in an optical fiber. In the case where a loss filter is desired, phase matching can be achieved between the fundamental mode and a cladding mode, which can then be stripped out to provide a narrow-band rejection filter [25]. LPGs have low insertion loss and high (20 dB) in-band rejection, making them suitable for inter-cavity isolation. However, unlike WDMs, which remove rejected light through a single-mode fiber, an LPG dumps rejected light into the fiber cladding, requiring careful thermal management at high-power operation. LPGs have also been demonstrated successfully as a means for isolating the ytterbium laser from the backward Stokes light [21].

Tilted fiber Bragg gratings (FBGs) are another potential possibility for isolating the rare-earth and Raman cavities. Unlike conventional FBGs, the index modulation that forms the grating is written at an angle with respect to the fiber core [15, 26]. In tilted FBGs, the reflected wavelengths are ejected from the side of the fiber, rather than backwards in the optical core. While tilted FBGs have not yet been used for cavity isolation in Raman fiber lasers, they have been demonstrated to remove other unwanted Stokes lines from a high-power Raman fiber laser [27].

It is worth noting that in architectures (described in more detail in later sections) that do not have a Raman cavity, such as cascaded Raman amplifiers [24] or integrated Yb–Raman architectures [28], the inter-cavity isolation is not necessarily required.

## 4. Design of Raman fiber lasers

In this section, we will briefly describe the modeling of conventional Raman fiber lasers. With minor changes, these equations can also be used to capture the more recent developments in the architectures for Raman lasers covered in the next section.

### *4.1. Numerical modeling of Raman fiber lasers*

In the cascaded Raman resonator, there is light at each of the intermediate Stokes wavelengths and in the input and the final wavelength. Using a subscript to denote the forward or backward nature, the equation for cascaded Raman lasers can be written as [17, 29]

$$\begin{aligned}\frac{dP_k^{b,f}}{dz} = {} & \pm\alpha_k P_k^{b,f} \mp \sum_{j<k}\frac{g_R(j,k)}{A_{\text{eff}}^j}(P_j^f + P_j^b)P_k^{b,f} \\ & \pm \sum_{j>k}\frac{\upsilon_k g_R(k,j)}{\upsilon_j A_{\text{eff}}^j}(P_j^f + P_j^b)P_k^{b,f} \\ & \mp \sum_{j<k}\frac{g_R(j,k)}{A_{\text{eff}}^j} h\upsilon_k \Delta\upsilon(\text{j})(P_j^f + P_j^b) \\ & \pm \sum_{j>k}\frac{\upsilon_k g_R(k,j)}{\upsilon_j A_{\text{eff}}^j} h\upsilon_j \Delta\upsilon(\text{j}) P_j^{b,f}.\end{aligned}$$

Here, $g_R(j, k)$ is the Raman gain coefficient which connects the $j$th and $k$th components. In conventional, single-wavelength Raman lasers, $j$ and $k$ differ by one (i.e., Raman gain for components separated by more than one Stokes component is negligible). However, as we will see later, in the case of multi-wavelength Raman lasers, the situation is more general. $A_{\text{eff}}^j$ is the effective area for the $j$th component and $\alpha_k$ is the fiber loss coefficient for the $k$th component. The transmission spectrum of the fiber can be incorporated through the fiber loss term. $\Delta\upsilon$ is the bandwidth of spontaneous emission needed to start the process and $\upsilon$ is the frequency of each wave. The above equations are generic and they incorporate both the forward and backward components. However, in some of the recent architectures, it is just sufficient to include the forward components. The same equations can be used with suitable modifications as appropriate. To solve the above equations, we need the boundary conditions. For the specific case of cascaded Raman resonators, the boundary conditions can be written as

$$P_k^f(0) = R_k^f P_k^b(0), \;\; P_k^b(L) = R_k^b P_k^f(L).$$

Here, $k$ represents the Stokes component with $k = 1$ being the pump and in an $n$ Stokes cascade the $n$th component will be the final signal. $L$ is the length of the Raman fiber. $R$ is the reflectivity provided by the fiber Bragg gratings. In a conventional cascaded Raman laser, all the reflectivities are close to unity except the two following components:

$$R_1^f = 0, \quad R_n^b = R_{\text{oc}}.$$

The first condition indicates that the pump is coupled straight into the cavity (there is no grating at the pump wavelength on the input side) and the second condition indicates that the final Stokes component has a lower-reflectivity output coupler (OC). The output power and efficiency are given by

$$P_{\text{out}} = (1 - R_{\text{oc}})P_n^f(L)$$

$$\eta = \frac{P_{\text{out}}}{P_{\text{in}}} = \frac{(1 - R_{\text{oc}})P_n^f(L)}{P_1^f(0)}.$$

### *4.2. Optimization of resonator components*

The above equations, in a general case, need to be solved numerically and the output parameters for a given set of conditions obtained. The goal is to maximize the efficiency of the Raman conversion process by tuning different laser parameters. Conventionally, the following parameters are tuned to maximize efficiency.

- *Fiber length.* At lower powers (<5 W), the length of fibers used can run to kilometers. This indicates the need for having low-effective-area (high-nonlinearity) fibers. With increasing powers this comes down, and at the 100 W level it can be lower than 100 m.
- *Grating reflectivity.* All the fiber gratings in the cascaded Raman resonator have reflectivities close to unity. The optimization is specifically aimed at the reflectivity of the output coupler. The reflectivity used will closely depend on the length of the fiber, the number of cascades in the Raman laser and the operating power. Enhanced reflectivity of the output coupler will result in lowering the threshold for the Raman laser. However, this also reduces the efficiency. Thus, a compromise must be made between operating at lower powers versus efficiency at higher powers. In high-power Raman lasers, it is common to have output coupler reflectivity less than 20%.
- *Grating bandwidths.* The long length of fiber used in Raman lasers results in line broadening of each of the Stokes components by processes such as four-wave mixing and self-phase modulation. The bandwidth of each of the gratings needs to be substantial enough to minimize light leakage around the bandwidth of the gratings. It is common to have bandwidths of more than 1 nm for the gratings used in the Raman resonator. However, with enhanced bandwidth of each grating, there is additional issues such as loss and reliability. Taking these factors into consideration, the bandwidth of each grating has to be optimized.

Detailed discussions on each of the above parameters and their optimization procedure can be obtained from [17].

In addition, when the Raman laser is built, a key requirement is to minimize the splice losses between the different fibers constituting the cavity. The laser has conventional or large-mode-area fibers in the rare-earth-doped laser, standard fibers in the fused fiber components such as the WDMs used for isolation and small-effective-area fibers in the Raman cavity. Further, there are several splices in each cavity, and with sub-optimal splices the loss can add up, resulting in significant deterioration of laser performance. Splicing between dissimilar fibers has been extensively researched [30], and sufficient care should be given to optimize all the splices before the laser can be assembled.

## 5. Recent developments: enhancement of efficiency, power, spectral quality and wavelength coverage of Raman lasers

### *5.1. Cascaded Raman lasers using filter fibers*

One significant limitation of early high-power Raman lasers operating at 1480 nm that used conventional Raman fibers in the Raman cavity was unwanted scattering into the next Stokes order at 1583 nm [19]. For example, for 125 m of Raman fiber in the cascaded Raman fiber laser (CRFL), the

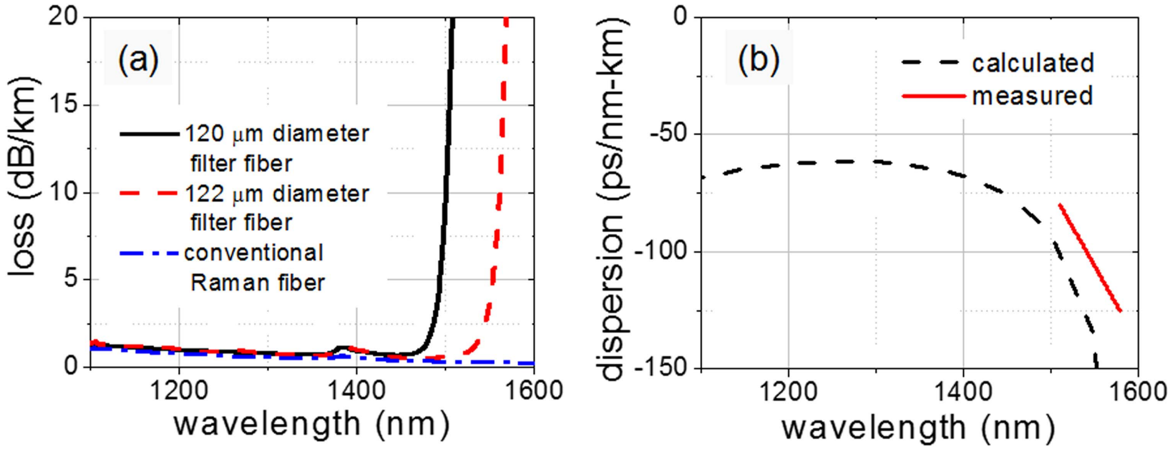


**Figure 10.** (a) Loss of the RFF compared to a conventional Raman gain fiber. (b) Calculated and measured dispersion of the RFF (from [21]).

1583 nm peak was only 15 dB below the 1480 nm peak at 41 W of output power. The 1583 nm peak could be reduced to 30 dB below the 1480 peak by shortening the fiber length to 65 m, but with a negative impact on conversion efficiency. Furthermore, as the fiber length was shortened, a smaller fraction of light at the output was contained at 1480 nm, with more residual radiation at the intermediate Stokes wavelengths, ultimately reducing the amount of output power at 1480 nm.

In order to maintain a long fiber length in the Raman cavity while suppressing scattering to the next Stokes order, a Raman filter fiber (RFF) was designed and fabricated. The RFF was a germanosilicate fiber that used a fundamental mode cut-off to achieve distributed loss at wavelengths longer than 1480 nm. Depressed clad fibers with fundamental mode cut-off have provided distributed loss for short-wavelength erbium-doped fiber amplifiers [31] as well as for Raman suppression in Yb-doped fiber lasers [32]. The RFF thus provides both cascaded Raman gain up to 1480 nm and distributed loss at longer wavelengths. The wavelength where the loss increases depends on both the scaling of the refractive index and the bend diameter. For example, an RFF was drawn to multiple diameters to find the fiber with the optimal cut-off wavelength. The measured loss curves of two different diameter RFFs are shown in figure 10(a), and compared to a conventional Raman gain fiber. At short wavelengths, from 1000 nm to 1480 nm, the losses of the RFF and conventional Raman fiber were similar, but at long wavelengths the RFF loss rapidly increased.

An additional consideration for fibers used in high-power Raman lasers is the dispersion of the Raman gain fiber over the operating wavelength range. If the dispersion of the Raman gain fiber were to become anomalous, modulation instability would lead to supercontinuum generation at high powers [33]. Therefore, the RFF must have normal dispersion over the entire operating range. As an example, a 1480 nm Raman fiber laser pumped by a 1050 nm Yb fiber laser requires normal dispersion from from 1050 nm to 1600 nm. The dispersion calculated for a normal dispersion filter fiber from the measured index profile of the fiber, as well as the measured dispersion, are shown in figure 10(b).

Although many Raman fiber lasers are based on germanosilicate fibers, a number of Raman lasers have recently been demonstrated using phosphosilicate fibers [33–37]. Phosphosilicate fibers have a peak Raman frequency shift of 40 THz compared to 13.2 THz in germanosilicate fibers; consequently only two Stokes orders are required to reach 1480 nm when using a Yb-doped fiber laser pump. Backward lasing off the first Stokes order is therefore not an issue, as the first Stokes wavelength in the phosphosilicate fiber is outside the Raman gain bandwidth of the Yb-doped fiber. Furthermore, in principle, when operating at 1480 nm the peak of the next Stokes shift in a phosphosilicate fiber would be at 1842 nm, where higher losses and larger mode area would give natural suppression of the next Stokes peak. In practice, however, the phosphosilicate fibers also have high Raman gain for small frequency shifts [35]. For example, a 2 km long, 10 W, 1240 nm phosphosilicate laser was limited by Raman lasing at 1330 nm. To date, Raman filtering has not been demonstrated in phosphosilicate fibers. However, filtering through distributed loss at high-power operation could be even more difficult in a phosphosilicate fiber than in a germanosilicate fiber due to the high gain that exists at small frequency shifts.

The introduction of RFFs into cascaded Raman lasers has led to considerable increases in output power from 1480 nm Raman fiber lasers. [21, 24, 38, 39]. In addition, because the distributed loss suppresses the unwanted scattering to the next Stokes order, the nonlinearity can be driven harder in a Raman cavity with filter fiber than in a comparable cavity based on conventional Raman fiber. As a result, Raman lasers based on filter fiber have higher efficiency and a higher fraction of in-band power compared to Raman lasers based on conventional Raman fiber. For example, for a pump power of 250 W, 81 W of 1480 nm output power was demonstrated [26] for an optical-to-optical conversion efficiency of 32% from a cavity with RFF. In comparison, a laser with conventional Raman fiber required 175 W of pump power for 41 W of 1480 nm output power or 23% conversion efficiency [17]. The increased conversion efficiency could be attributed to the RFF, which allowed long lengths of Raman fiber to be used without being limited by scattering to 1590 nm.

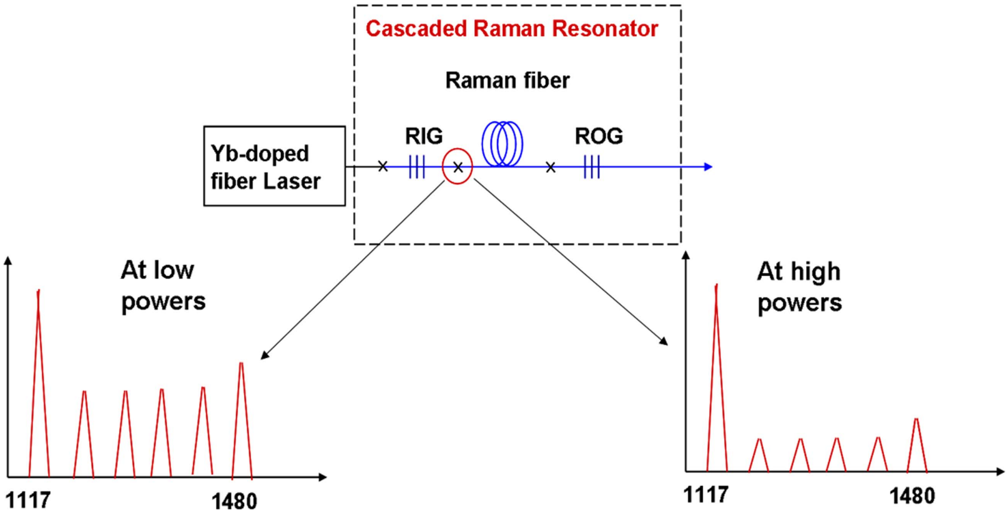


**Figure 11.** Qualitative representation of spectra near the input for a fifth-order cascaded Raman fiber laser at lower and higher powers.

### *5.2. High-efficiency Raman lasers using cascaded Raman amplifiers*

The efficiency of the cascaded Raman lasers is still substantially lower than the fundamental quantum-limited efficiency despite the improvement with the filter fiber. Here, a new architecture will be described which achieves a substantial enhancement in conversion efficiency.

The reduction in efficiency in conventional cascaded Raman lasers can be identified as occurring due to the following reasons.

1. Linear losses in the Raman input grating set (RIG) and output grating set (ROG) [9].
2. Potentially high-loss intra-cavity splices between low-effective-area (possibly dissimilar) fibers constituting the grating sets and the Raman gain fiber.
3. Transmission loss due to scattering and absorption in the Raman fiber.
4. Enhanced backward and forward light leaking from the cavity at the intermediate wavelengths due to their bandwidth being higher than the grating bandwidths [17, 29, 40].
5. Splice losses occurring in the high-power path in the laser such as the Yb-doped fiber laser to Raman fiber splice.

Most of the loss mechanisms identified above occur as part of the cascaded Raman resonator assembly. Figure 11 shows a schematic diagram of the spectral content of light at the start of the cascaded Raman resonator. Such a measurement can be made by analyzing the light scattered at the splice spectrally. At low powers, it is observed that there is a sizable fraction of light at all intermediate Stokes wavelengths. However, at higher powers this fraction reduces considerably. This suggests that, instead of a resonator, a single-pass cascaded Raman amplifier can work equally well for high-power Raman lasers as long as it is sufficiently seeded at all the intermediate Stokes wavelengths. Seed powers at all the intermediate wavelengths reduces the gain requirement, provides wavelength selectivity and enables preferential forward Raman scattering. Using a pump separated by more than one Stokes shift from the signal with the wavelength conversion mediated by intermediate wavelengths has been used previously used in optical communications for applications in Raman amplifiers and in remote pumping of Er-doped fiber amplifiers [41, 42].

For the single-pass cascaded Raman amplifier, two key constituents are necessary. The first is a preferably simple multi-wavelength source which can simultaneously provide sufficient powers at all the intermediate wavelengths. A lower-power conventional cascaded Raman laser lends itself ideally to this purpose. Light present at the output at all the intermediate Stokes wavelengths provides sufficient seed power at the required wavelengths. Second, scattering of the output wavelength to the next Stokes order can be higher in a single-pass configuration compared to a cascaded resonator configuration. The use of RFF eliminates this problem and provides an ideal technique to terminate the cascade of wavelength conversion. Figure 12(a) shows the experimental setup based on the new architecture. A high-power Yb-doped fiber laser is combined with a lower-power Raman seed laser (spectrum shown in figure 12(b)). This is then sent through a gain medium such as Raman fiber or RFF (an example transmission spectrum shown in figure 12(c)). The need for a filter fiber is more stringent in this case to stop additional scattering of the output light to the next Stokes order.

Figure 13 shows the results from an experiment to utilize the cascaded Raman amplifier architecture to develop a fifth-order converter from 1117 nm to 1480 nm. The total output power and the 1480 nm component as a function of input power at 1117 nm are shown in figure 13(a). An output power of ~301 W at 1480 nm is achieved (limited only by input power) for a total input power of ~470 W (including the Yb-doped fiber laser in the seed source) with a total conversion efficiency of ~64% (1117 nm to 1480 nm, quantum-limited efficiency of 75%). Taking into account the efficiency of the Yb-doped fiber laser, an optical-to-optical conversion

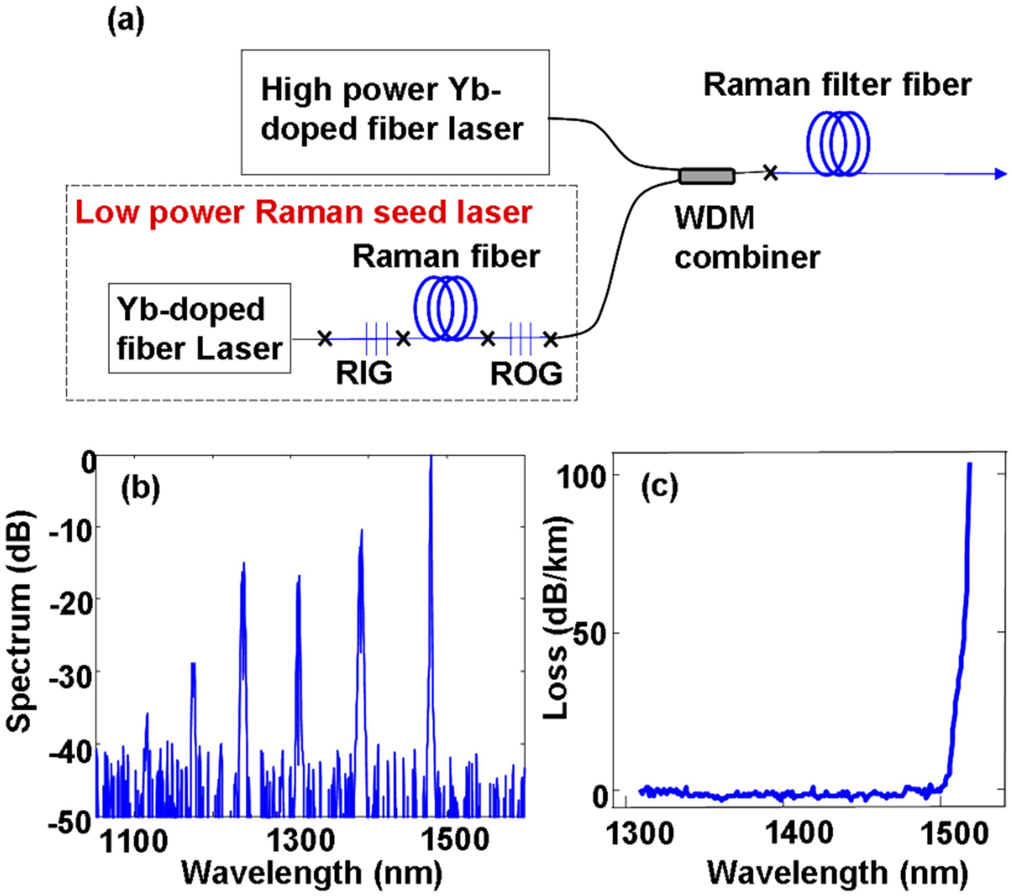


**Figure 12.** (a) Schematic diagram of the single-pass cascaded Raman fiber amplifier architecture. (b) Spectrum of the low-power seed source. (c) Transmission spectrum of the RFF (from [24]).

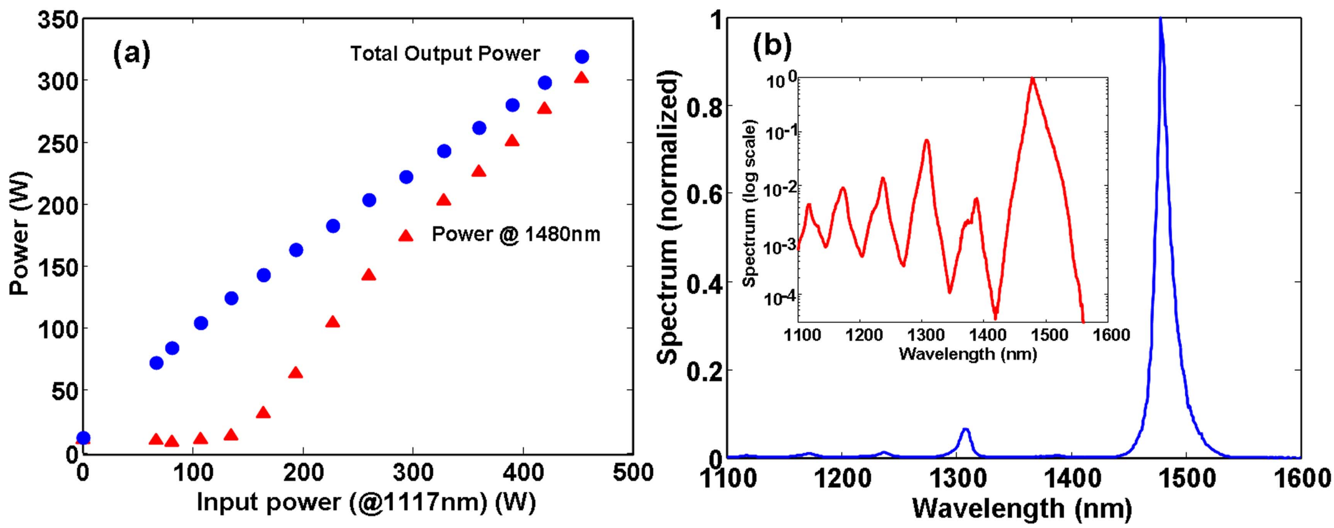


**Figure 13.** (a) Output power and component at 1480 nm for a fifth-order cascaded Raman amplifier laser. (b) Output spectrum (in linear and log scale) (from [24]).

efficiency from 975 nm pump to 1480 nm signal of ~42% is achieved. A comparison to this system would be the alternate methods to develop high optical powers in the 1.5 $\mu$m wavelength region using erbium–ytterbium co-doped fiber lasers. The conversion efficiency in [3] was less than 25% and decreasing due to parasitic lasing. Further enhancement of the ytterbium laser efficiency can increase the total laser efficiency [43]. Figure 13(b) shows the measured output spectrum at full power (log scale in the inset). More than 95% of the power is in the 1480 nm band, indicating a high level of wavelength conversion, while high suppression of the next Stokes order at 1590 nm is maintained through the use of the

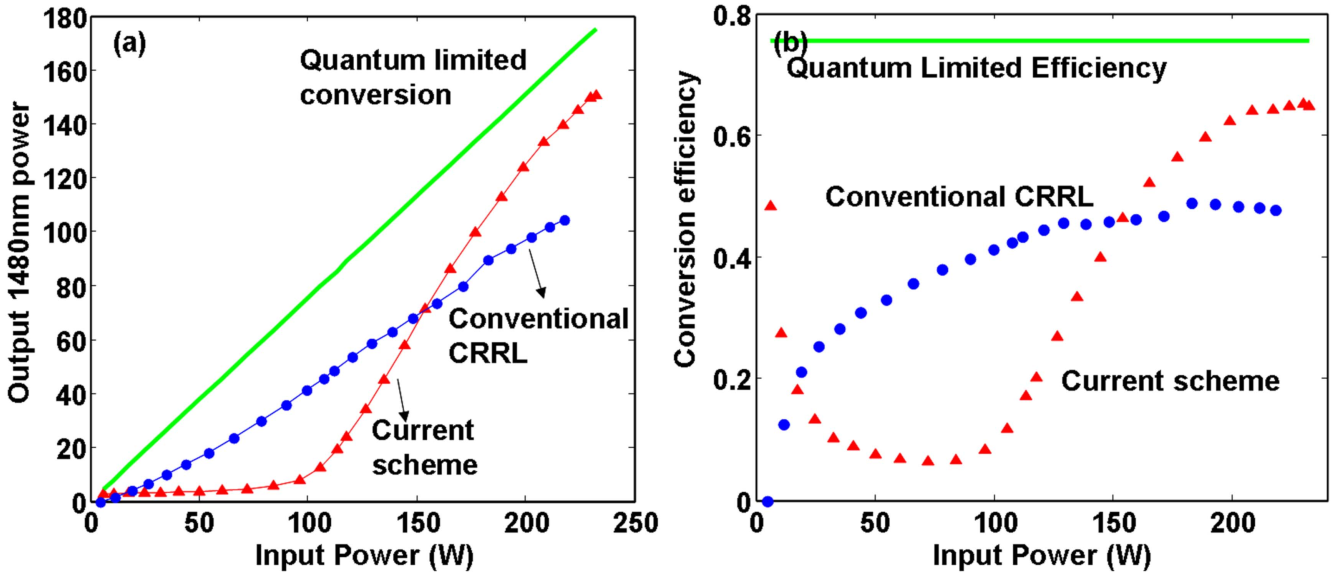


**Figure 14.** (a) Comparison of the input power to the output power for different cascaded Raman laser architectures. (b) The corresponding conversion efficiencies (from [39]).

filter fiber. The reduction in efficiency below the quantum limit can be accounted for by the loss of the WDM combiner, splices and residual power in the other Stokes components, giving clear directions.

To illustrate the enhancement in efficiency compared to the conventional architecture, the results obtained from this scheme [39] are compared to previous results in [38] where 104 W at 1480 nm was obtained. To obtain optimal efficiencies at lower maximum input powers, the length of the RFF was adjusted. The power from the seed source in this experiment is ~3 W at 1480 nm and 4 W in total. Figure 14(a) compares the output power at 1480 nm for the two architectures together with the quantum-limited efficiency (calculated w.r.t. the input power at 1117 nm). At lower powers, power from the new scheme is low since the cascade is not driven all the way to 1480 nm. However, once the threshold is reached, the power rapidly grows and at full power is significantly higher than that from the conventional cascaded Raman laser. At the maximum power point for the conventional Raman laser, the new scheme provides 40% more power. Figure 14(b) shows the corresponding conversion efficiencies. At low power, the current scheme's output is dominated by the seed source and has the corresponding ~48% conversion efficiency. With increasing powers, but prior to threshold, this efficiency drops, but quickly recovers beyond this and achieves a maximum of ~65%. It is necessary to point out here that the efficiency of a conventional cascaded Raman laser is power dependent as well (the optimal length of Raman fiber in the resonator needs to be modified), and the results plotted above from [38] achieve close to maximum efficiency at the highest power levels.

To demonstrate the function of the cascaded Raman amplifier more intuitively, figure 15 shows the total output power and components at each Stokes wavelength measured as a function of input power at 1117 nm to the cascaded amplifier. Interpolation has been used between the measured data points to better represent the evolution of powers. A progressive growth and decay of all the intermediate Stokes components with increasing power is clearly observed. A rapid growth of the final output wavelength is seen beyond a power threshold. The filter fiber ensures there is no further conversion of the output wavelength. At maximum power, a high degree of wavelength conversion, with most of the output power being in the final, 1480 nm component, is seen. The initial offset of the 1480 nm component (and the total power) is due to the seed source. An interesting behavior with the penultimate Stokes component (1390 nm) is seen, which is unlike the previous ones. The presence of significant power already at the output wavelength (1480 nm) manifests as additional loss through stimulated Raman scattering for the 1390 nm component. This creates a more complicated growth and decay condition. This behavior can become the limiting factor on power of the seed source. If the 1480 nm component

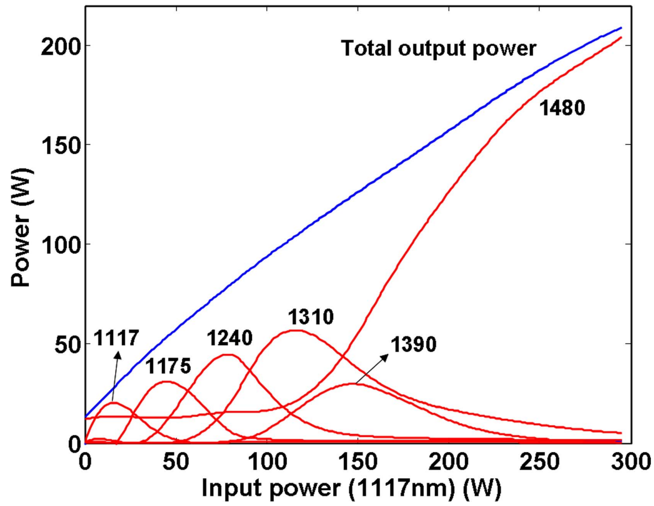


**Figure 15.** Experimental measurement (from spectra) of different components of the cascade as a function of input power (from [39]).

is too powerful, it can prematurely deplete the 1390 nm component, suppressing the power transfer from 1310 nm. This can result in incomplete wavelength conversion and reduced efficiency. The modeling necessary to analyze the cascaded Raman amplifier configuration is further described in [24].

### *5.3. Hybrid rare-earth–Raman lasers*

One challenge for power scaling of Raman fiber amplifiers is to combine a high-power pump laser with a seed laser. In standard configuration, WDMs are used for the combination. They are single-mode components, whose capability in sustaining high power is limited. Recent reports had proven that throughput of a few hundred watts is feasible [24, 44, 45], but further power scaling to kilowatt level has not yet been demonstrated. On the other hand, pump and signal combiners have been widely used in high-power rare-earth-doped fiber lasers [1]. In these components, the pump fibers are multimode, which allows higher power input. Power scaling of a single-mode Yb-doped fiber amplifier to 20 kW has been demonstrated with a pump and signal combiner.

Integrating rare-earth and Raman fiber devices was proposed as a way to scale the Raman fiber amplifier above kilowatts [46]. To do this, standard high-power Yb-doped fiber amplifiers are seeded with multiple lasers, whose wavelength separations are close to the Raman shift. The seed laser with the shortest wavelength is at the middle of the Yb gain spectrum, which is amplified efficiently. The laser power is then transferred to the longer wavelengths successively in the subsequent optical fiber by stimulated Raman scattering. The most important improvement in the architecture is the elimination of the WDM that has been used in almost all high-power core-pumped Raman fiber lasers. Here the Raman seed lasers and pump laser are propagated and amplified in the core of the same fiber.

In a proof of principle experiment [46], a 300 W all-fiber linearly polarized single-mode amplifier at 1120 nm was demonstrated with an optical efficiency of 70%, limited only by available pump power. The amplifier consists of 4 m of ytterbium-doped fiber and 20 m of passive fiber, and is seeded with a laser emitting at 1070 and 1120 nm. The gain fiber has a cladding diameter of 125 $\mu$m and a core diameter of 10 $\mu$m.

As proofs of the power scalability of the proposed architecture, experiments with gain fibers of larger cladding were carried out. Fibers with larger cladding allow higher power input of the diode laser pump. With gain fibers of 400 $\mu$m cladding and 10 $\mu$m core, an up to 580 W single-mode linearly polarized Raman fiber laser at 1120 nm was achieved, with an optical efficiency of 70% [47]. The 1120 nm laser purity at maximum power is 95%. The experimental setup is shown in figure 16. The 10 $\mu$m core fiber guarantees diffraction-limited output. The large cladding-to-core area ratio of 40 reduces the absorption coefficient of Yb-doped fiber. Therefore, Yb-doped fiber 25 m long was used in the experiments. With such long gain fiber, no extra Raman fiber after the Yb gain fiber is necessary, because the Raman conversion is already sufficient within the Yb gain fiber. Furthermore, with gain fibers of 400 $\mu$m cladding and 20 $\mu$m core, a 1.3 kW Raman fiber laser at 1120 nm was generated, which is the first report of a Raman fiber laser with over a kilowatt output [48].

Shortly after this, the output from such an integrated Yb–Raman fiber amplifier was increased to 1.5 kW with higher pump power [48]. The idea was also applied to the mid-infrared (IR) wavelength range. By integrating Tm and Raman fiber amplifiers, 14.3 W output at 2147 nm was reported [50]. Since all current high-power rare-earth-doped fiber lasers have a master oscillator power amplifier scheme, the proposed architecture can be applied conveniently and further scales the Raman fiber laser output and extends the spectral coverage.

### *5.4. Narrow-linewidth Raman fiber lasers and amplifiers*

The obvious advantage of Raman fiber lasers and amplifiers is wavelength agility. However, many wavelength sensitive applications also require narrow linewidth. In some cases, further nonlinear frequency conversion processes, such as second-harmonic generation and sum frequency mixing, are necessary to achieve the target wavelength. These processes also require narrow-linewidth sources.

A narrow-linewidth, single-longitudinal-mode laser has been reported with distributed feedback (DFB) Raman fiber lasers [51, 52], which will be discussed in a later section. Direct generation of a high-power narrow-linewidth laser from usual Raman fiber oscillators formed by two FBG reflectors is difficult. Raman gain is relatively low as compared with rare-earth gain, so Raman fiber lasers usually have longer fiber cavity. Nonlinear processes, such as four-wave mixing, would broaden the laser linewidth in square-root law when the laser power is increased [53, 54]. Nevertheless, high-power narrow-linewidth lasers can be generated by fiber Raman amplification of single-frequency seed lasers. The seed lasers are usually DFB or external cavity diode lasers, which also can emit over an ultra-wide spectral range.

The development in narrow-linewidth Raman fiber amplifiers has been driven by a particular application in astronomy, called sodium laser guide star adaptive optics [45, 55]. For this application, a high-power narrow-linewidth laser at 1178 nm is needed, which is frequency doubled to 589 nm.

Figure 17 shows a typical 1178 nm narrow-linewidth Raman fiber amplifier configuration. Backward pumping is necessary to preserve narrow linewidth, since dramatic linewidth broadening can be observed in forward-pumped Raman fiber amplifiers. The effective nonlinear path length in forward-pumped amplifiers is substantially higher than in backward-pumped amplifiers, resulting in the enhanced line broadening. The pump wavelength, 1120 nm, is selected to match the Raman shift in silica fiber. A 1120/1178 nm WDM is used to couple the pump light into the backward-pumped single-mode Raman fiber amplifier. Two more 1120/1178 nm WDMs are inserted between the seed laser and amplifier to extract the remaining pump laser and protect the seed laser.

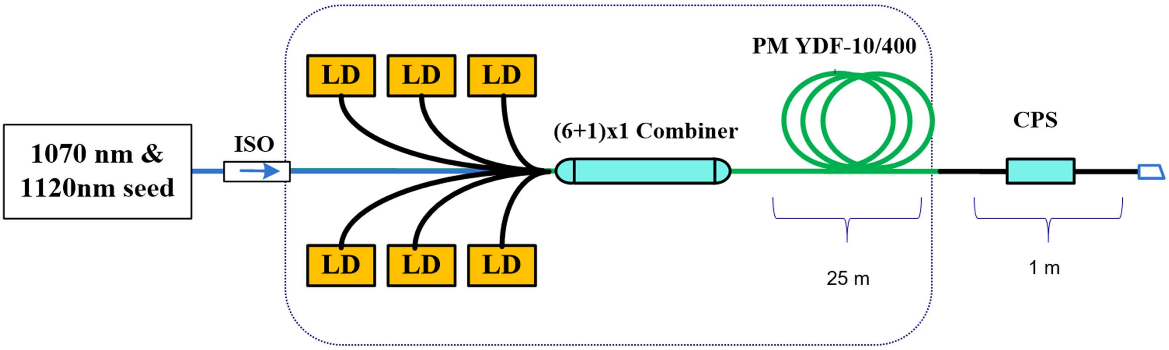


**Figure 16.** Schematic diagram of an integrated Yb–Raman fiber amplifier.

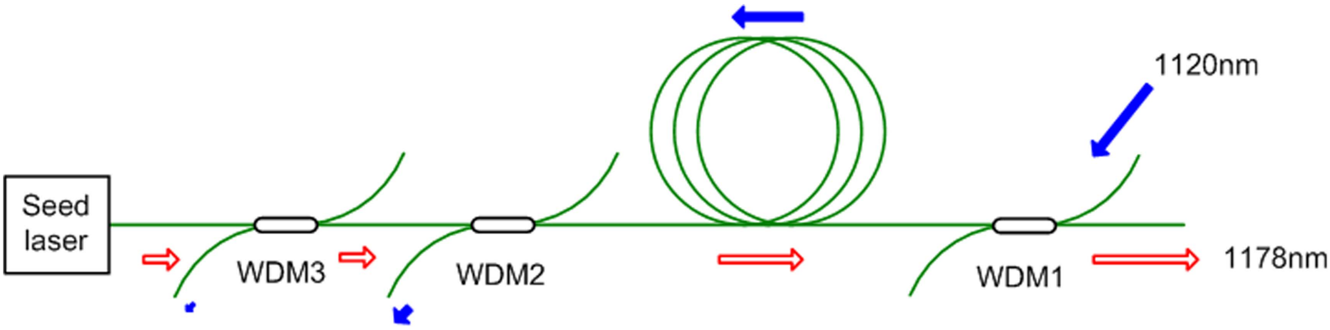


**Figure 17.** Typical experimental setup of a 1178 nm Raman fiber amplifier pumped by a 1120 nm fiber laser.

Stimulated Brillouin scattering (SBS) is the main limiting factor in high-power narrow-linewidth Raman fiber amplifiers, because the Brillouin gain coefficient is two order of magnitude higher than the Raman gain coefficient [56]. As long as the SBS reaches threshold, the laser is downshifted and propagates backward towards the seed laser. This not only limits the amplification, but also destabilizes the amplifier.

Although the Brillouin gain coefficient is two orders of magnitude higher than the Raman gain coefficient, 10% efficiency amplification of a megahertz linewidth 1178 nm laser was demonstrated [57]. The reason behind this is that the power distribution of the laser inside the Raman fiber amplifier is uneven, close to exponential in the reported experimental condition. Most laser power is generated in a short piece of fiber at the end of the amplifier. Therefore, the effective fiber length for the SBS process is much shorter than the amplifier fiber length. Moreover, numerical simulation shows that the SBS-limited output is proportional to the pump power [58]. One can increase the amplifier output by raising the pump power.

However, to improve the amplifier efficiency, SBS has to be suppressed. One way to suppress the SBS is to broaden the seed laser linewidth [57, 59], which however is not wanted for many applications. Another way is to broaden the SBS gain spectrum, which includes many methods.

Acoustically tailored fibers had been explored to reduce the Brillouin gain, while maintaining or even enhancing Raman gain [60, 61]. This is achieved through the manipulation of the concentration of dopants in the core as a function of position in the transverse direction. Up to 22 W single-frequency 1178 nm output was obtained in a backward-pumped two-stage amplifier with an optical efficiency of about 25% [61]. The same group of researchers also reported suppression of SBS by applying thermal gradients along the gain fiber, and achieved 1.5-fold improvement in a single-stage amplifier experiment [62]. Similarly, cascading multiple pieces of different fibers and multiple isolated amplifier stages can be used to increase the Brillouin threshold [57, 61]. However, the scalability of these methods is limited.

The most successful method of suppressing SBS in narrow-linewidth Raman fiber amplifiers until now is to apply longitudinally varied strain along the gain fiber. This has been studied since the 1990s in the telecom community [63, 64]. The strain introduces a proportional shift of the SBS gain spectrum. Therefore, with a strain distribution, SBS light from different portions of the gain fiber is spectrally isolated and cannot be amplified efficiently in other portions of the fiber. Application of the technique to narrow-linewidth Raman fiber amplifiers has been investigated extensively since 2003 [58, 65–68], and described in the literature [45, 58, 69, 70].

In high-gain Raman fiber amplifiers, the power varies along the gain fiber steeply. The strain distribution has to be carefully designed according to the power distribution to achieve desirable SBS suppression. Figure 18 shows a typical design of step-wise strain distribution for a Raman fiber amplifier, in which a 1 W seed laser is amplified to 30 W and 10 strain steps are implemented in the 35 m long gain fiber. The fiber length for different strain steps varies significantly. This is very different from the suppression of SBS in a

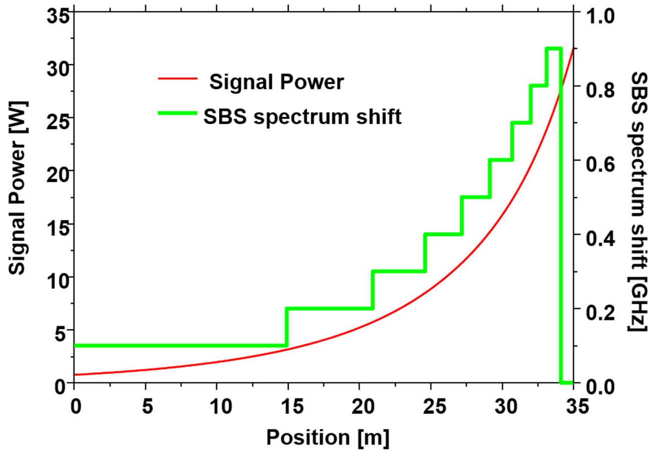


**Figure 18.** Typical design of a 10-step strain distribution for a Raman fiber amplifier.

passive delivery fiber, where uniform strain steps are close to the optimum.

With the strain methods, the highest conversion efficiency reported is 52% [69]. In that work, an up to 44 W, 1 MHz linewidth, 1178 nm continuous wave (CW) laser is obtained by Raman amplification of a DFB diode laser in a variably strained polarization maintaining fiber pumped by a linearly polarized 1120 nm fiber laser. 30 strain steps were applied in the amplifier, and a 20-fold reduction in the effective SBS coefficient was achieved. In later reports [45, 47], 84 W CW and 120 W peak power microsecond-pulsed single-frequency Raman fiber amplifiers were demonstrated. These results represent the highest output reported for single-frequency Raman fiber amplifiers.

### *5.5. Mid-IR Raman fiber lasers*

Fiber lasers operating in the mid-IR spectral range have applications in LIDAR, gas sensing, and optical communications. Conventional optical fibers made using silica are not transparent in the mid-IR wavelengths and novel materials are necessary. Optical fibers made with soft glasses, such as fluoride and chalcogenide, are candidates as efficient gain media for mid-IR laser generation, because they have low phonon energy and are transparent in the mid-IR [71]. $Ho^{3+}$-doped ZBLAN fiber lasers had been reported at 2.85, 3.22, and 3.9 $\mu$m. 2.8 and 3.5 $\mu$m emissions from $Er^{3+}$-doped ZBLAN fiber lasers were reported. $Dy^{3+}$-doped ZBLAN fiber lasers at 2.9 $\mu$m have also been reported.

Raman fiber lasers or amplifiers are an alternative way to generate mid-IR fiber lasers, with the additional advantage of wider wavelength tunability. A 3.7 W fluoride glass Raman fiber laser operating at 2231 nm has been reported [12]. A single-mode $As_2S_3$ cascaded Raman fiber laser emitting at 3.77 $\mu$m was demonstrated based on nested Fabry–Perot cavities formed by two pairs of FBGs [13]. This is the longest wavelength reported so far for Raman fiber lasers. Numerical simulation of $As_2S_3$ Raman fiber lasers was carried out, showing that they have potential in generating the entire 3–4 $\mu$m spectral band [72].

While mid-IR Raman lasers with soft glass fibers show great potential, it remains technically challenging to extend the spectral coverage and increase the output power. The soft glass fibers are mechanically weak, and therefore require careful handling. The laser damage threshold is low, and therefore power scaling is difficult. The unavailability of common fiber components, such as FBGs and WDMs, places more difficulty in building mid-infrared Raman fiber devices. Owing to these reasons, there has been recent work on trying to push conventional silica fiber-based lasers to longer wavelengths. The key issue as mentioned previously is that the propagation loss of light increases steeply in silica fiber when the wavelength is longer than 2.2 $\mu$m.

Highly Ge-doped silica fibers have been used to generate >2.1 $\mu$m Raman lasers, because they have higher Raman gain coefficient and comparatively lower attenuation [50, 73, 74]. In 2008, Rakish *et al* reported silica fiber Raman emission at wavelength as long as 2.41 $\mu$m with an output of 24 mW, which was achieved via spontaneous cascaded Raman amplification [75].

The idea was later explored further into the longer-wavelength edge of silica fiber by another group of researchers [76]. With a pulsed 2.008 $\mu$m Tm fiber laser as pump source, a maximum second Raman–Stokes power of 0.30 W at 2.43 $\mu$m was achieved with an optical efficiency of 16.5% and a peak power of 275 W. In the case of 2.04 $\mu$m pumping, a maximum power of 0.15 W at 2.48 $\mu$m was achieved with an optical efficiency of 7.9%. Because highly Ge-doped silica fiber can be easily spliced to standard silica fibers, higher-power 2 $\mu$m $Tm^{3+}$- or $Ho^{3+}$-doped fiber lasers can be used as a pump source to increase the amplifier output in an all-fiber configuration. The results show that Raman lasers or amplifiers with highly Ge-doped silica fiber as gain media might be valuable sources for the 2.1–2.5 $\mu$m spectral range, which is one of the atmospheric transmission windows. Considering the availability of high-sensitivity detectors, the 2–2.5 $\mu$m band is still the most important mid-IR transmission window of the atmosphere for remote sensing applications [77].

## 6. Novel implementations of Raman fiber lasers

### *6.1. Multi-wavelength Raman fiber lasers*

In the discussions so far, the output wavelength of the Raman laser has been a single, fixed wavelength. However, there are applications which requires a multi-wavelength Raman laser. Specifically, in Raman amplifiers, using multiple pumps spaced in wavelength from each other results in a flatter gain profile. Multi-wavelength Raman lasers achieve this by having resonant cascaded cavities at two or more different output wavelengths. The pump source is the same and often the first few cascades are also the same. However, at later cascades, using the broad bandwidth of the Raman gain, two or more different cavities are fabricated. This involves having multiple closely spaced HR gratings and HR, OC gratings in the RIG and ROG sets respectively. Multi-wavelength Raman lasers having up to six different wavelengths have been demonstrated so far [78, 79]. The equations governing the multi-wavelength Raman lasers are the same as for the single-wavelength Raman laser with additional components added for each of the new wavelengths. Owing to multiple competing processes for gain in these lasers, comprehensive analysis is important before fabrication work of these lasers can be undertaken.

### 6.2. Cladding-pumped Raman fiber lasers and amplifiers

The cladding pumping technique has revolutionized fiber laser technology in power scaling. Cladding pumping is a natural progression of Raman fiber devices as well as providing further power increase. The cladding-pumped Raman fiber amplifier was first discussed by Nilsson *et al* in 2002 [80]. In contrast to core-pumped Raman fiber lasers, the cladding-pumped Raman fiber laser emits light with higher brightness than the pump laser, which is an important property of conventional lasers. To gain a large brightness enhancement, high cladding-to-core area ratio is preferred. However, if the cladding-to-core area ratio is too large, the intensity generated in the core can greatly exceed that in the cladding long before the pump laser is depleted. This leads to the generation of parasitic second-order Stokes light in the core, limiting the conversion from pump light to first-order Stokes light [81]. To increase the conversion efficiency, the area ratio between the inner cladding and core has to be less than about eight [82, 83], which then limits the actual enhancement of brightness.

A specially designed filter fiber as discussed previously can be used to improve the cladding-to-core area ratio. The filter fiber has sharp spectral characteristics. Parasitic Raman conversion to the second-order Stokes light can be suppressed by bending loss, while the loss at the first-order Stokes light is kept low. The ratio between the inner-cladding area and the effective area of the Stokes wave can be improved: up to 40 was shown to be feasible [81, 84]. Cascaded cladding-pumped, cascaded Raman fiber lasers, or amplifiers with multiple-clad fiber were also proposed as gain medium to overcome the inner-cladding-to-core area ratio restriction [85]. The low-brightness pump light is coupled into the second cladding (first inner cladding) of the fiber; Raman–Stokes light is generated in the third cladding. Similarly, the generated Stokes light will act as pump light and generate the higher-order Stokes light in the fourth cladding. The processes happen in a cascade until the single-mode laser is generated in the fiber core. By designing the neighboring claddings with small area ratio (for example, less than 8), the parasitic Stokes laser could be suppressed. Therefore, the restriction on the cladding-to-core area ratio can be removed by introducing the intermediate claddings.

### 6.3. Raman DFB and DBR lasers

Typically, the output linewidth of high-power Raman lasers is relatively broad, on the order of a nanometer at modest powers, and several nanometers or more at 50 or 100 W of power. However, lasers with narrow linewidths have many applications in remote sensing, spectroscopy, frequency conversion, and coherent combination of multiple fiber laser sources.

One approach to narrowing the linewidth of a Raman laser is to use a distributed Bragg reflector (DBR) structure, with a short length of Raman fiber between two Bragg gratings [86–89]. For example, by reducing the cavity length to 12 m, the output FWHM of the Raman laser could be reduced to 170 pm for 11 W of intra-cavity power, even though the cavity supported 10 000 longitudinal modes [88, 89]. However, correlations between the modes led to temporal dynamics. By further reducing the cavity length to 17 cm, a cavity was obtained that supported only 24 longitudinal modes [86], with a lasing threshold as low as 400 W, and a linewidth of 60 pm at 700 mW output power. Unfortunately, even with such a low number of longitudinal modes, it was found that the linewidth broadened substantially to 328 pm at 4.3 W, when the short DBR laser was used as a seed source for a power amplifier (MOPA configuration) [87].

For narrow-linewidth operation, then, a cavity that supports only a single longitudinal mode is highly beneficial. A DFB fiber laser, first demonstrated in 1994 [90], consists of a fiber Bragg grating inscribed in an active fiber waveguide. Fiber DFB lasers are thus a convenient approach to obtaining single-frequency optical fiber sources. However, until recently, all-fiber DFBs relied on rare-earth doping, typically erbium or ytterbium, to provide the gain medium.

An interesting possibility is to combine a DFB structure with Raman gain to create a single-frequency Raman fiber DFB laser operating at wavelengths unattainable with rare-earth elements. The possibility of a Raman fiber DFB laser was first discussed by Perlin and Winful in 2001 [91]. These authors considered a uniform 1 m long fiber Bragg grating without a $\pi$ phase shift. Using a linear analysis they showed that the threshold could be below 1 W. To compute the laser output they reported a full time domain solution of the nonlinear coupled mode equations including the grating, Kerr nonlinearity, and the Raman effect. A more recent study by Hu and Broderick [92] considered a uniform 20 cm cavity with a $\pi$ phase shift offset from the center of the grating. Their simulations gave a threshold close to 1 W and a slope efficiency of 80%. Although the Raman gain per unit length is small ($\sim$0.01 dB $m^{-1}$ $W^{-1}$), because of the high $Q$ of the cavity, the intra-cavity signal can be strong enough to cause significant depletion and thus effective usage of the pump. The offset phase shift made the lasing more efficient and unidirectional, as in the case of rare-earth-doped DFBs [93]. A subsequent study by Shi and Ibsen [94] considered the effect of grating imperfections on the lasing characteristics, showing that such lasers should be robust to phase and amplitude noise imposed on the grating profile.

The first demonstration of a Raman fiber DFB laser was in 2011 [52, 95]. In this demonstration, the pump laser was a high-power 1480 nm Raman fiber laser. The SMF pump output was spliced to a 1480/1550 nm WDM, which was then spliced to the DFB fiber, to observe backward lasing power. The Bragg wavelength of the DFB was 1583 nm. The

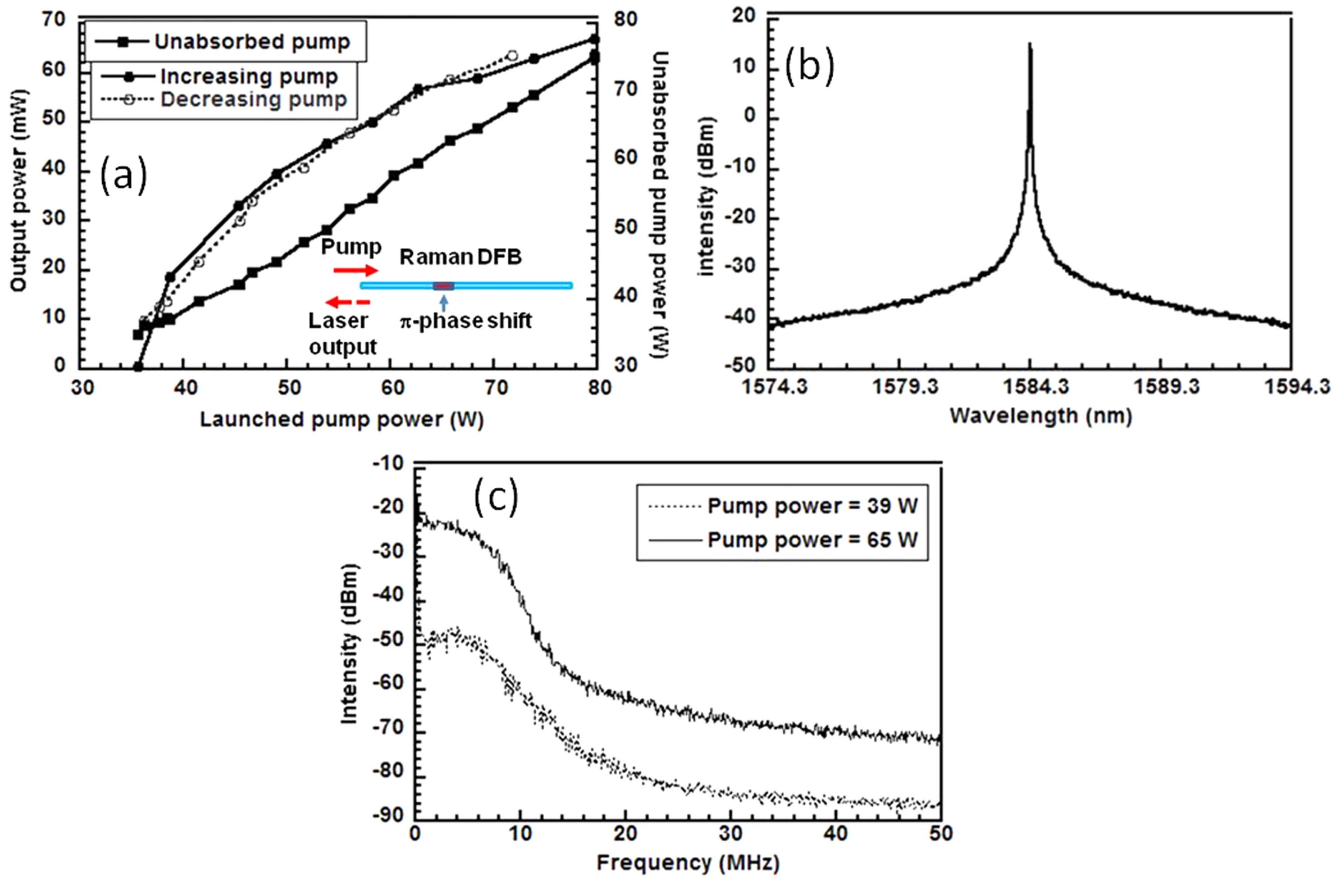


**Figure 19.** Measurements from the first demonstration of a Raman fiber DFB laser. (a) Output power and unabsorbed pump power as a function of launched pump power. (b) Output spectrum showing lasing at 1584.3 nm. (c) Delayed self-homodyne measurement of the laser linewidth. (From [52]).

DFB was written in OFS Raman fiber with NA = 0.23, effective area 18.7 $\mu$m$^2$ (at 1550 nm), cut-off $<$ 1050 nm, and Raman gain efficiency for unpolarized light of 2.5 W km$^{-1}$. The Raman gain fiber length was 14 cm with roughly 21 cm on either side of the grating. The grating profile was uniform and a $\pi$ phase shift (an offset in the periodicity of the grating creating the DFB cavity) was placed 8% off center at 71.92 mm. The backward output of the laser was coupled to test and measurement equipment. Optical measurement results from the laser are shown in figure 19. Figure 19(a) shows the output power versus pump power. Very little pump power was absorbed, making the pump power at the output of the laser very large compared to the laser signal output. Additional filtering was not sufficient to measure the forward power of the laser accurately. Thus the laser was oriented to lase in the backward direction toward the WDM. Because of the large amount of unabsorbed pump power, the threshold pump power was very high (35 W) and maximum output power was only 65 mW.

Figure 19(b) shows the spectrum measured with an optical spectrum analyzer, and figure 19(c) shows the result of a self-homodyne measurement of the laser linewidth, confirming a narrow linewidth of 6 MHz.

Shortly after this initial demonstration of a Raman fiber DFB laser, additional Raman DFB results were reported, substantially improving on the performance [51, 96]. In this work, a Yb fiber laser operating in the 1 $\mu$m wavelength region nm was used, compared to the 1480 nm Raman fiber laser used in ref [52]. DFB gratings were written in germanosilicate fibers, and it was found that in a fiber with a high NA of 0.35 the lasing threshold was as low as 1 W of pump power, and the maximum output power was up to 1.6 W for slightly less than 13 W pump. Furthermore, the slope efficiency with respect to the absorbed pump was found to be close to the quantum limit. With subsequent optimization of the DFB, the threshold was reduced to 440 mW, and the laser linewidth was less than 2.5 kHz [96]. These results indicated the promise for Raman fiber DFB lasers at wavelengths unavailable from rare-earth-doped fibers.

In this section, so far, a fabricated Bragg grating has been used to create DFB in each of the lasers. Alternately, random feedback in a long length of optical fiber can be used to create a DFB cavity. Such a long cavity in conjunction with Raman gain has been utilized to develop random DFB Raman lasers [97]. In this work, over 150 mW of signal light at 1555 nm was demonstrated, pumped with 2.5 W at 1455 nm. However, owing to the absence of strong spectral filtering in the cavity, the laser is still not narrow linewidth (single longitudinal mode) as in the Bragg DFB cases.

### 6.4. Raman lasers utilizing gas-filled optical fibers

In conventional Raman lasers, solid fibers are utilized and the Raman gain is largely limited by the materials commonly used. Gases are an attractive alternative for Raman gain since they differ not only in the frequency shifts but also in the linewidth of the Raman interaction. This has been made use of to develop Raman lasers using gas-filled optical fibers. In [98], a hollow core photonic crystal fiber was filled with hydrogen and a Raman laser was demonstrated. Pumped at 1064 nm, several watts of output power at the Stokes wavelength of 1135 nm was demonstrated. This was improved to output powers of over 55 W in [99].

In addition to hydrogen, deuterium [100], hydrogen Cyanide and acetylene [101] have also been used.

## 7. Some applications of Raman fiber lasers

### 7.1. Frequency conversion

Cascaded Raman shifting of a Yb-doped fiber laser can generate lasers at any wavelength between 1.1 and 1.6 $\mu$m [24, 102]. By second-harmonic generation in nonlinear optical crystals, the Raman fiber laser can be converted to the visible range. The orange and red wavelength range is particularly interesting, because it cannot be reached by rare-earth-doped solid state lasers [103].

The sodium laser guide star in astronomy has played an important role in motivating the development of high-power Raman fiber amplifiers [20, 55]. It requires a high-power narrow-linewidth 589 nm laser to excite a layer of sodium atoms 90 km high in the atmosphere, to generate an artificial 'guide star'. With its help, the image distortion induced by atmosphere turbulence can be compensated with adaptive optics technology [104]. The laser guide star technology is essential for large-aperture telescopes to approach the designed angle resolution.

In early days, rhodamine dye lasers at 589 nm were used for sodium guide stars. However, dye lasers are difficult to maintain. Solid state 589 nm lasers were researched for replacement. The sum frequency mixing of two Nd:YAG laser lines at 1064 nm and 1319 nm happens to be 589 nm. Over the years, high-power 589 nm Nd:YAG lasers with different formats, such as CW, mode locked, long pulsed etc, have been demonstrated and fabricated [105–108]. However, they were still too bulky and complicated for operation in remote astronomical sites. Therefore, fiber-based sodium guide star lasers have been pursued. Among different technical paths, the Raman-fiber-amplifier-based guide star laser is the most advanced at present.

The high-power narrow-linewidth 1178 nm Raman fiber laser can be converted to 589 nm by a single pass in periodically poled nonlinear crystals [109–111]. However, the conversion efficiency is below 30% in the investigated power level, and a practical source by this method remains below 10 W for the reliability of the periodically poled nonlinear crystals.

Practical 589 nm guide star lasers can be generated in LBO crystals, which have much higher laser damage thresholds. LBO crystals have lower nonlinear coefficient, therefore they are placed in an enhancement cavity. The enhancement cavity usually has a bow-tie configuration. By optimizing the input mirror reflectivity and mode matching optics, a single-frequency 1178 nm laser can be coupled into the enhancement cavity efficiently after cavity length locking. Figure 20 shows a resonant doubling cavity in action. A laser with a maximum of 57 W at 589 nm has been reported, with a conversion efficiency of 80% [45, 69, 112, 113]. A 20 W-class sodium guide star laser product is also available [114, 115], and has been successfully installed in the VLT of ESO [116] and Keck Observatory in Hawaii [117].

There are numerous applications for yellow–orange–red lasers. The 589 nm narrow-linewidth laser can also be used for laser cooling of sodium atoms [118]. At a slightly different wavelength of 588 nm, it can be used for precision spectroscopic measurement of helium [119]. For these applications, the required power is a few watts. Therefore, simple single-pass frequency doubling in periodically poled nonlinear crystals is adequate [109, 120]. There are also applications in medical treatment, for example ophthalmology and dermatology, which do not have strict requirements on laser linewidth. In these cases, Raman oscillators are favorable than Raman master oscillator power amplifiers, because of their simplicity. The linewidth broadening effect usually seen in Raman fiber oscillators sets a challenge in improving the frequency doubling efficiency, because the periodically poled nonlinear crystals have a narrow wavelength acceptance bandwidth [105, 115].

### 7.2. Raman lasers for optical pumping

High-power Raman fiber lasers can be used as effective sources for optical pumps for other, rare-earth-doped fiber lasers or amplifiers. The wavelength versatility of the Raman fiber laser means that it can be used for high-power pumping of optical absorptions at wavelengths which are difficult to achieve with other means such as direct diode pumping or rare-earth-doped fiber lasers. Furthermore, the single-mode output from the Raman laser can enable core pumping, or high-brightness cladding pumping. Core pumping with Raman lasers is especially attractive for pulsed fiber laser systems, where core pumping helps keep the active fiber length short even with relatively low-absorption fibers, which is important for high-peak-power or high-pulse-energy systems.

Er-doped fiber lasers have lagged behind Yb-doped fibers in power scaling. Nevertheless, there is significant interest in high-power erbium-doped fibers due to the relative eye safety of the 1.5 $\mu$m wavelength range, compared to operation at 1 $\mu$m. Furthermore, a window of atmospheric transparency at 1.5 $\mu$m makes the Er-doped fiber laser attractive for applications involving free-space operation, such as remote sensing, LIDAR and free-space communications. The highest power demonstrated to date from a fiber laser at 1.5 $\mu$m was from an ErYb laser. An output power of 297 W was obtained

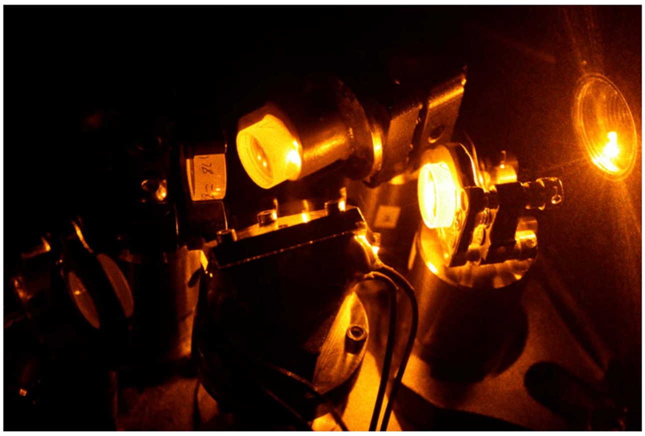

**Figure 20.** Frequency doubling in an enhancement cavity.

at 1.56 $\mu$m for a pump power of 1.2 kW at 975 nm, but the slope efficiency and further power scaling were limited by parasitic lasing of the Yb ions at 1.06 $\mu$m [3]. High-efficiency in-band core pumping of ErYb has also been reported using a 1535 nm fiber laser as a pump, but the maximum output power was limited to 18 W [121].

As a result of difficulties in power scaling ErYb fibers, there has been recent interest in power scaling of Yb-free Er fiber lasers. One approach to high-power operation of Yb-free Er fiber lasers is direct cladding pumping with multi-mode 976 nm diode lasers [122–124]. The maximum power achieved to date using direct diode cladding pumping of a Yb-free, Er-doped fiber is 100 W [124]. Another approach is to cladding, in-band pump either Yb-free Er, or ErYb fiber, using multi-mode 15xx pump diodes, or fiber lasers [125–127]. One difficulty with diode pumping with 15xx diodes is that they are not as well developed, or high performance, as multi-mode diodes operating at 976 nm. The highest power reported to date from a single-mode Yb-free Er fiber in-band, cladding pumped with diodes is 88 W [125].

In comparison, a single-transverse-mode Er fiber laser core pumped by a high-power, 1480 nm Raman fiber laser has also generated over 100 W of output power [128]. A schematic diagram of the laser setup, plot of output power versus launched pump power, and plot of the output optical spectrum are shown in figure 21. Because of the core-pumping configuration, a standard telecom single-mode Er fiber, OFS MP980, could be used as the active gain medium. Although OFS MP980 has a low Er absorption, a relatively short length of 21 m of fiber could be used due to the core-pumping architecture. Furthermore, the low dopant concentration helps reduce clustering, resulting in the high slope efficiency of 71% with respect to launched pump power. Finally, using a cascaded Raman pump distributes the heat load due to the quantum defect among multiple stages (Yb laser, cascaded Raman resonator, and Er laser) compared to direct diode pumping of an erbium laser. This heat load distribution helps to ease thermal management.

*7.2.1. Core pumping of pulsed, Er-doped amplifiers with high-power 1480 nm Raman lasers.* While using Raman lasers to pump CW Er lasers has generated over 100 W output power, Raman lasers are also advantageous for pulsed applications. For example, at moderate power levels, a cascaded Raman fiber laser can provide several watts of pump power to generate tens of nanojoules of pulse energy from an all-normal dispersion, femtosecond mode-locked fiber oscillator using a single-mode Er fiber [129].

In order to scale pulse energies and peak power significantly beyond what can be achieved with a single-mode fiber, the effective area of the mode in the Er fiber needs to be increased substantially. In this regime, Raman fiber lasers and the core-pumped architecture have some distinct additional advantages. As mentioned previously, core pumping helps keep the fiber length short, compared with cladding pumping, which is important for increasing nonlinear thresholds such as self-phase modulation, Brillouin scattering, and Raman scattering. Furthermore, Yb-free, Er fibers more readily lend themselves to large-mode-area (LMA) fibers with diffraction-limited performance [6], as the relatively simple composition aids in fabricating precision refractive index profiles. Finally, in fibers that support multiple modes, but are intended to operate on only a single mode, the high pump/signal overlap in a core-pumped architecture provides suppression of unwanted higher-order modes via differential gain [130, 131]. One negative aspect of core pumping is that experiments and simulations have shown lower efficiency in core-pumped ErYb amplifiers, compared with cladding-pumped amplifiers, due to a lower pump intensity mitigating pair-induced quenching [132].

A general schematic diagram of a very large-mode-area amplifier architecture pumped by a 1480 nm Raman fiber laser is shown in figure 22. In such an amplifier, the pulsed signal and the high-power 1480 nm Raman laser are coupled together with a 1480/1550 single-mode fiber wavelength division multiplexer. Pump and signal are then launched together into the fundamental mode of the very large-mode-area (VLMA) Er amplifier, where amplification takes place.

Direct amplification of picosecond pulses in an approximately 3 m long VLMA amplifier with 1100 $\mu$m$^2$ effective area has been demonstrated to peak powers of ~127 kW [6]. Femtosecond, chirp-pulse fiber amplifiers using Raman-pumped VLMA Er fibers have also been demonstrated. In a germanosilicate 4.5 m long VLMA fiber with effective area of ~875 m$^2$, 25 J 800 fs pulses were demonstrated [133]. More recently, using a 28 cm long, Er-doped phosphate glass with effective area of 2290 $\mu$m$^2$ and pumped by a Raman laser, sub-500 fs pulses with a pulse energy of 915 $\mu$J were demonstrated [134]. The large mode area of VLMA fibers combined with high-power Raman pumps also makes them well suited to systems that require both high average power and high peak power. 100 W average power, 10 GHz, 130 fs pulses with diffraction-limited beam quality were generated from a 3 m long VLMA Er fiber with effective area of

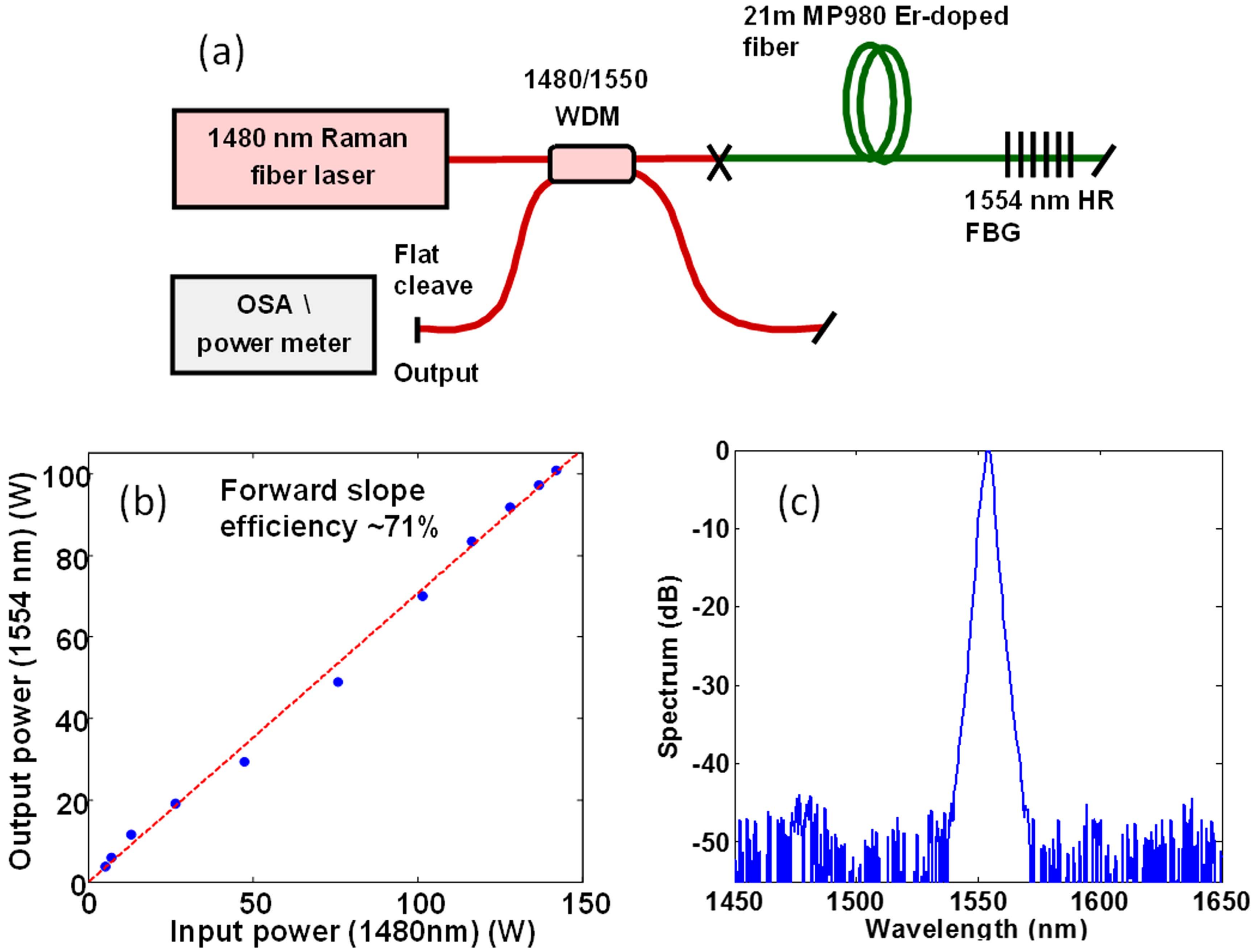


**Figure 21.** 100 W, CW Er laser pumped by a high-power Raman laser. (a) Laser setup. (b) Output power versus pump power. (c) Output optical spectrum. (From [128].)

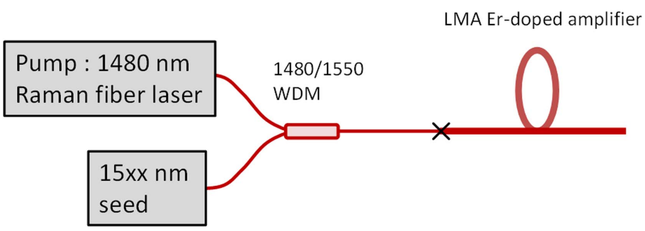


**Figure 22.** General schematic diagram of a large-mode-area Er-doped amplifier pumped by a high-power, 1480 nm Raman fiber laser.

1100 $\mu m^2$ [135]. The optical performance of this system is illustrated in figure 23.

For further scaling of effective area and pulse peak power beyond what a VLMA fiber can achieve, a specially designed higher-order mode (HOM) fiber can be used [136]. HOM fibers are few-moded fibers designed to operate on a single higher-order mode, typically the $LP_{0,N}$ mode. In an HOM amplifier, the signal is launched into the fundamental mode of the fiber. A long-period grating (LPG) then provides phase matched coupling to the desired $LP_{0,N}$ HOM. In the case of an Er HOM amplifier pumped by a single mode Raman laser, both pump and signal are launched into the same HOM [137], providing almost perfect overlap between pump and signal, and conferring the benefits of core pumping discussed above. At the output of the amplifier the signal can be converted to a diffraction-limited beam either with a second matched LPG, or in the case of a high-peak-power system with a bulk-optic mode converter such as an axicon [138]. Er-doped HOM amplifiers have been demonstrated with effective areas as large as 6000 $\mu m^2$ [139]. A schematic diagram of a typical Er-doped HOM amplifier, pumped by a Raman fiber laser, is illustrated in figure 24. An important benefit of HOM fibers is that they are less susceptible to bend-induced area reductions compared to fundamental mode fibers [140].

Comparison between Er VLMA and Er HOM amplifiers in femtosecond CPA systems has shown that the achievable pulse energy scales with the effective area of the mode, whether the mode is a fundamental mode or higher-order mode [138]. In a high-power CPA system based on a Raman-fiber-laser-pumped, Er-doped higher-order mode fiber, sub-500 fs pulses of 300 $\mu$J were achieved [141]. This particular system used an LPG for output mode conversion, which adds nonlinearity to the overall system. Thus a system using a

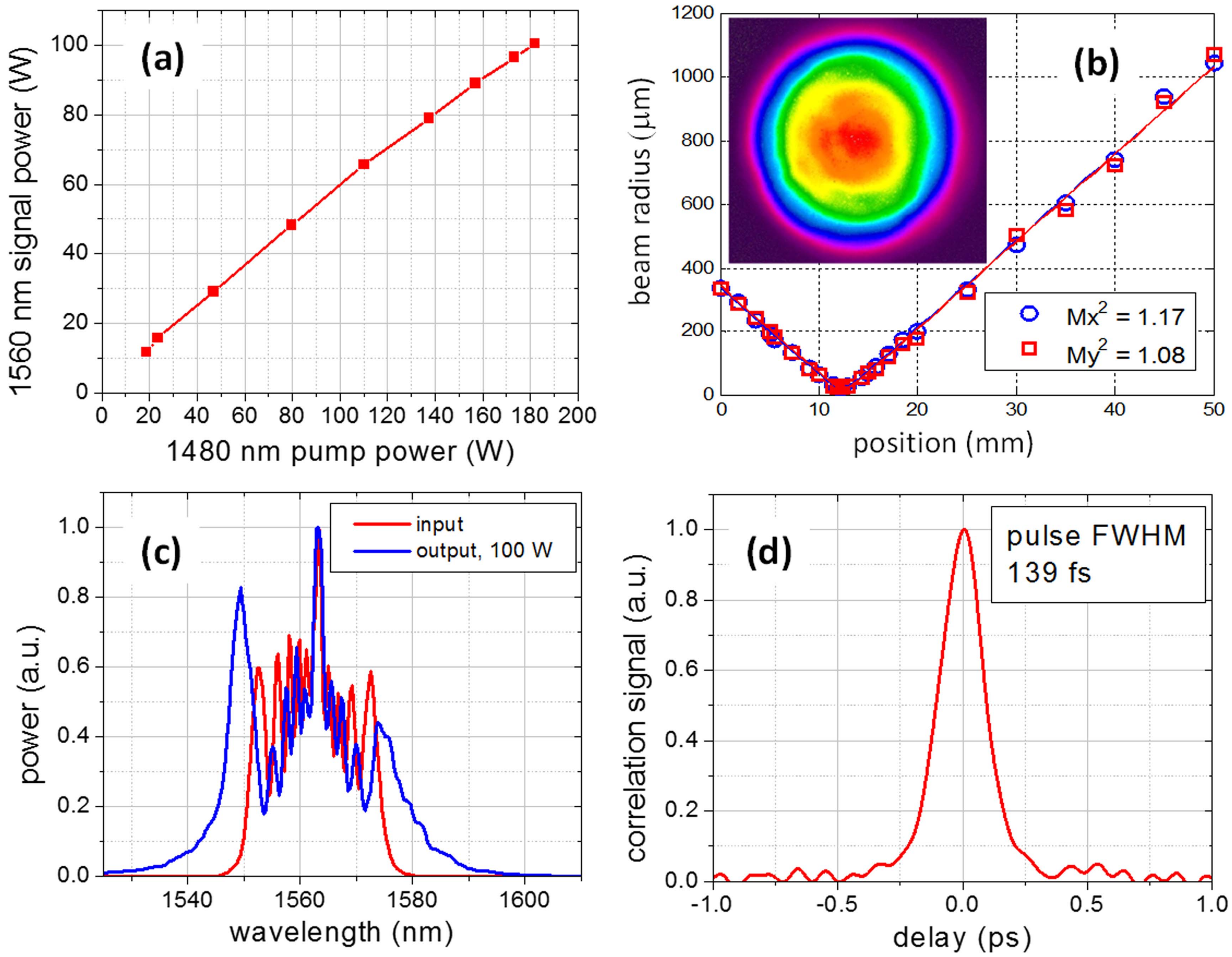


**Figure 23.** Amplification of 10 GHz, femtosecond pulses in a VLMA Er amplifier pumped by a high-power 1480 nm Raman laser. (a) Output power versus pump power. (b) Beam quality at 100 W output power. (c) Amplifier input spectrum and output spectrum at 100 W power. (d) Autocorrelation at 100 W output power. (From [135].)

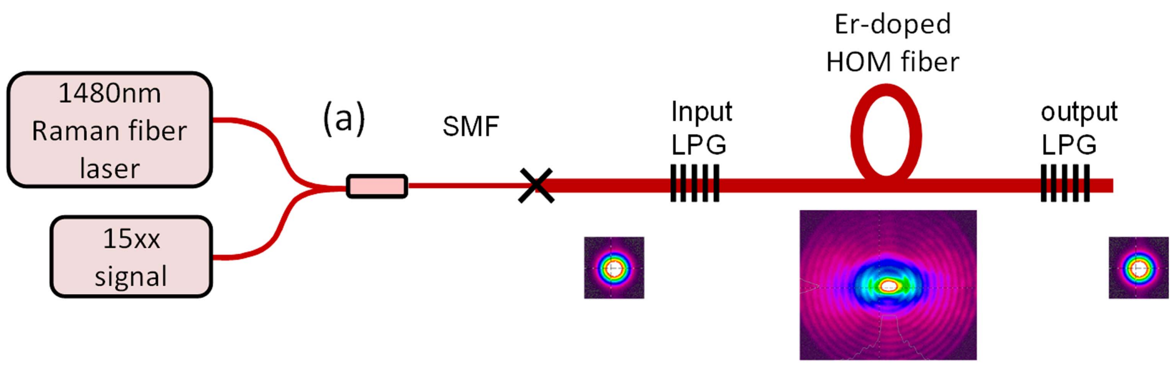


**Figure 24.** Er-doped HOM amplifier pumped by a 1480 nm Raman fiber laser.

bulk-optic axicon for mode conversion would be expected to provide further pulse energy scaling.

The large effective area of the Er-doped HOM fiber is also advantageous for direct amplification of nanosecond pulses up to 700 kW peak power [142]. Finally, the large effective area of the HOM, together with high anomalous dispersion, is ideal for generating self-frequency-shifted solitons in a Raman-laser-pumped amplifier. 186 nJ, 91 fs solitons, tunable from 1570 nm to 1620 nm, with a peak power of 1.9 MW, were demonstrated from an Er HOM amplifier pumped by a Raman laser, compared to 17 nJ, 106 fs from a VLMA Er fiber [143].

*7.2.2. 2 $\mu$m and 3 $\mu$m fiber lasers pumped by Raman lasers.* In addition to Er fiber lasers at 1.5 $\mu$m, fiber laser sources operating at 2 $\mu$m and 3 $\mu$m provide another interesting route to high power at an eye-safe wavelength. Holmium-doped and thulium-doped fiber lasers are both promising candidates for high-power 2 $\mu$m and 3 $\mu$m radiation. For both of these types of fiber laser, there are a number of potential pumping schemes [144]. Th fiber lasers are often pumped at 790 nm with laser diodes, 1560 nm with Er fiber lasers, or tandem pumped at 1.9 $\mu$m with short-wavelength Th fiber lasers. Pumping schemes for Ho fiber lasers include 1.95 $\mu$m with Th fiber lasers or 1.15 $\mu$m with long-wavelength Yb fiber lasers.

Alternatively, Raman fiber lasers have been demonstrated as a pump source for both Th and Ho fiber lasers. Two 1173 nm Raman fiber lasers generating up to 230 W were used to cladding pump a Th-doped fiber laser to generate more 96 W of output power [145]. An 1150 nm Raman fiber laser with 110 W of output power was used to pump a Ho-doped fiber laser to generate 42 W of output power near 2048 nm [146]. 1150 nm Raman fiber lasers have also been used to pump Ho-doped ZBLAN fibers to generate 3 $\mu$m fiber lasers [147, 148].

### 7.3. Optical communications

Raman fiber lasers have applications in optical communications as pump sources. More generally Raman amplification, whether the pump source is a Raman fiber laser or a diode laser, is used in optical communications to provide gain in order to counteract the loss from long transmission spans of optical fiber, as well as other optical components in the communications system.

Raman amplifiers in telecom systems are often classified into two categories: distributed amplifiers and discrete amplifiers. In distributed amplification [149–151], Raman gain is used advantageously in the optical fiber transmission spans that provides transport of the optical signals. In long-haul communication systems, these fiber spans can be 100 km or longer. By adding distributed amplification the noise of the system is improved by increasing the signal level at the receiver without having to increase the launched signal power (which can increase system nonlinearities).

In contrast, discrete amplifiers are ones where Raman gain is provided by shorter fibers other than the transport fiber. The most common example of this is the discrete Raman amplifiers that make use of the Raman gain in dispersion compensating fiber (DCF) [152–154]. DCFs provide compensation of the chromatic dispersion that is accrued in the optical span. They are shorter in length than the fiber used in the span (typically at most a few kilometers long), but they are also smaller in effective area, and as such provide higher Raman gain.

To provide Raman gain in a telecom fiber, whether a discrete or a distributed amplifier, a pump source at a wavelength one Stokes shift below the signal wavelength is launched into the fiber span. The pump laser could be another Raman fiber laser, or a high-power diode laser.

To generate the broad bandwidth gain required for modern high-channel count optical communications systems, multiple pump wavelengths are required to broaden the Raman amplifier gain beyond what can be achieved with a single pump wavelength. Pump sources for such amplifiers could be a bank of wavelength division multiplexed pump diodes [155], or a single Raman fiber laser operating simultaneously on multiple wavelengths [78, 79], which can be achieved through careful selection of the fiber Bragg grating wavelengths.

For example, a broadband telecom Raman amplifier, using 12 diode laser pumps with wavelengths from 1400 nm to 1520 nm, with flat gain over bandwidth of 100 nm and gain ripple less than 0.1 dB over 80 nm has been demonstrated [155]. In order to achieve such a result, careful design of the pump wavelengths and relative intensities is required, to account for the pump–pump interactions that naturally occur in such an amplifier [156].

By separating the various pump wavelengths in time, the pump–pump interactions in a multi-wavelength Raman amplifier can be suppressed [155]. This approach, also known as time division multiplexed Raman pumping, can achieve broad bandwidth Raman gain with extremely low gain ripple and reduce other impairments such as pump-induced four-wave mixing [158, 159].

As mentioned above, the pump wavelengths in a typical Raman amplifier for optical communications are one Stokes shift separation from the signal wavelength. This configuration is also known as first-order pumping. Another configuration is second-order pumping, where an additional pump wavelength is used one Stokes shift below the first-order pump wavelength [160]. For example, if the signal wavelength is 1550 nm, the first-order pump would be at approximately 1460 nm, and the second-order pump would be at 1370 nm. By using second-order pumping, gain in long hauls spans can better distributed through the fiber length such that the signal power does not reach as low a minimum as with first-order pumping. As such, the use of second-order pumping can improve the signal-to-noise ration in distributed Raman amplifiers.

The literature on Raman lasers and Raman amplifiers in optical communications is extensive. Substantial work has gone into development of Raman amplifiers and overcoming issues encountered such as polarization dependence of Raman gain [161]. For a more in-depth review of Raman amplifiers in optical communications please see [162] and [17].

### 7.4. CW supercontinuum generation with Raman fiber lasers

Supercontinuum lasers are an important technology which has found applications in a variety of fields [163, 164]. Commonly referred to as 'broad as a lamp, bright as a laser' they are particularly useful for imaging, test and measurement and spectroscopic applications. High-power fiber supercontinuum lasers are generated by pumping a nonlinear medium with a high-power fiber laser in the anomalous dispersion region close to the zero dispersion point. Modulation instability coupled with four-wave mixing, soliton generation and Raman scattering each play a crucial role in the supercontinuum generation [163, 164]. Line broadening is also observed in the normal dispersion region; however, this is a substantially weaker effect and pumping in the normal dispersion region cannot generate a supercontinuum. Optical fibers owing to low loss and long interaction lengths provide ideal nonlinear media for supercontinuum generation. However, silica fibers, which are used primarily, have strong normal dispersion in the 1050 to 1120 nm wavelength region. For this reason, high-power supercontinuum generation has been primarily demonstrated using microstructure fibers [165]. With microstructure fibers, an all-fiber architecture is difficult to achieve due to problems with splicing, and free-space coupling is used. Further, the technology is still relatively recent, and widespread adoption as in the case of silica fibers is not yet there.

Silica fibers on the other hand have anomalous dispersion at wavelengths longer than 1310 nm. In particular, at the 1550 nm region, mature component technology is available due to applications in optical communications. Highly nonlinear fibers [166] with high nonlinear coefficients and zero dispersion are available in this band, which is ideal for supercontinuum generation. However, there is a lack of suitable sources for pumping. Raman lasers provide an excellent method to wavelength convert high-power Yb-doped fiber lasers to the zero dispersion region of the highly nonlinear fibers and generate broadband, high-power supercontinua. In [167, 168], a highly nonlinear fiber with zero dispersion at 1480 nm was pumped by a 1117–1480 nm Raman laser to generate over 3 W of power and a 20 dB bandwidth of over 500 nm spanning from 1200 nm to 1700 nm. In recent years [169] there have been attempts to improve the architecture and performance of these supercontinuum sources.

### *7.5. Raman fiber lasers for biological tissue coagulation*

Here, we briefly describe a recent biological application of Raman lasers in tissue coagulation. The ability of Raman lasers to emit high powers at any wavelength enables development of high-power lasers to interact with media resonantly at their absorption lines, in this case biological tissue. By developing a high-power fiber laser at 1.44 $\mu$m, in [170], the investigators were able to selectively coagulate and ablate tissue (porcine esophagus, *ex vivo*). Absorption by water in the tissue is responsible for the resonant interactions at 1.44 $\mu$m. Currently, there is no rare-earth doped fiber laser which directly emits at 1.44 $\mu$m. We anticipate this ability of Raman fiber lasers to emit at any arbitrary wavelength to become important for various biological applications in the coming years.

## 8. Summary

In this review, we introduced the technology of Raman fiber lasers focused on the developments that are recent. In particular, we looked at new topics such as using filter fibers to enhance efficiency of Raman lasers, high-efficiency, cavity-less architectures for Raman lasers, mid-IR Raman lasers and narrow-linewidth Raman lasers. We also looked at a small subset of Raman laser applications in the areas of laser pumping, optical communications, frequency conversion and biology.

From the discussions above, we believe it is sufficiently clear that Raman fiber lasers are a wavelength agile, scalable, high-power fiber laser technology. It is anticipated that this agility will further enhance the importance of Raman lasers in the coming years. Extensive research and development efforts to further advance this technology and to meet new application requirements that emerge is absolutely essential.

## Acknowledgments

V R Supradeepa would like to thank Santosh Aparanji, V Balaswamy and S Arun for help with the organization and useful suggestions on the manuscript.

## References

[1] Richardson D J, Nilsson J and Clarkson W A 2010 High power fiber lasers: current status and future perspectives [Invited] *J. Opt. Soc. Am.* B **27** B63–92
[2] Ehrenreich T, Leveille R, Majid I, Tankala K, Rines G and Moulton P 2010 1 kW, all-glass Tm:fiber laser *Proc. SPIE* **7580** 758016
[3] Jeong Y *et al* 2007 Erbium:ytterbium codoped large-core fiber laser with 297 W continuous-wave output power *IEEE J. Sel. Top. Quantum Electron.* **13** 573
[4] https://lia.org/publications/ansi/Z136–1
[5] Clark R N 1999 Spectroscopy of rocks and minerals, and principles of spectroscopy *Manual of Remote Sensing* vol 3 (Wiley) Remote Sensing for the Earth Sciences
[6] Jasapara J C *et al* 2009 Diffraction-limited fundamental mode operation of core-pumped very-large-mode-area Er fiber amplifiers *IEEE J. Sel. Top. Quantum Electron.* **15** 3–11
[7] Grubb S G *et al* 1994 High power, 1.48 $\mu$m cascaded Raman laser in germanosilicate fibers *OSA Topic. Meeting, Optical Amplifiers and Their Applications*
[8] http://fiber-optic-catalog.ofsoptics.com/item/optical–fibers/raman-optical-fiber1/raman-fiber
[9] Reed W A, Stentz A J and Strasser T A 1998 Article comprising a cascaded Raman fiber laser *US Patent* 5, 815, 518
[10] Genty G, Coen S and Dudley J M 2007 Fiber supercontinuum sources *J. Opt. Soc. Am.* **24** 1771
[11] Babin S A, Churkin D V, Ismagulov A E, Kablukov S I and Podivilov E V 2007 Four-wave-mixing-induced turbulent spectral broadening in a long Raman fiber laser *J. Opt. Soc. Am.* **24** 1729–38
[12] Fortin V, Bernier M, Faucher D, Carrier J and Vallée R 2012 3.7 W fluoride glass Raman fiber laser operating at 2231 nm *Opt. Express* **20** 19412–9
[13] Bernier M, Fortin V, El-Amraoui M, Messaddeq Y and Vallée R 2014 3.77 $\mu$m fiber laser based on cascaded Raman gain in a chalcogenide glass fiber *Opt. Lett.* **39** 2052–5
[14] Chen M, Shirakawa A, Fan X, Ueda K-I, Olausson C B, Lyngsø J K and Broeng J 2012 Single-frequency ytterbium doped photonic bandgap fiber amplifier at 1178 nm *Opt. Express* **20** 21044–52

[15] Kashyap R 1999 *Fiber Bragg Gratings* (Academic)
[16] Kashyap R 2013 The fiber fuse—from a curious effect to a critical issue: a 25th year retrospective *Opt. Express* **21** 6422–41
[17] Agrawal G and Headley C 2005 *Raman Amplification in Fiber Optical Communication Systems* (Elsevier)
[18] Dianov E M and Proghorov A M 2000 Medium-power CW Raman fiber lasers *IEEE J. Sel. Top. Quantum Electron.* **6** 1022
[19] Emori Y, Tanaka K, Headley C and Fujisaki A 2007 High-power cascaded Raman fiber laser with 41 W output power at 1480 nm band *Conf. on Lasers and Electro-Optics/Quantum Electronics and Laser Science Conf. and Photonic Applications Systems Technologies, OSA Technical Digest Series (CD)* (Optical Society of America) paper CFI2
[20] Feng Y, Taylor L R and Calia D B 2009 150 W highly-efficient Raman fiber laser *Opt. Express* **17** 23678–83
[21] Nicholson J W, Yan M F, Wisk P, Fleming J, DiMarcello F, Monberg E, Taunay T, Headley C and DiGiovanni D J 2010 Raman fiber laser with 81 W output power at 1480 nm *Opt. Lett.* **35** 3069–71
[22] Kawasaki B S, Hill K O and Lamont R G 1981 Biconical-taper single-mode fiber coupler *Opt. Lett.* **6** 327–8
[23] Agrawal G P 1997 *Fiber-Optic Communication Systems* 2nd edn (Wiley Interscience)
[24] Supradeepa V R and Nicholson J W 2013 Power scaling of high-efficiency 1.5 μm cascaded Raman fiber lasers *Opt. Lett.* **38** 2538–41
[25] Vengsarker A M, Lemaire P J, Judkins J B, Bhatia V, Erdogan T and Sipe J E 1996 Long-period fiber gratings as band-rejection filters *IEEE J. Lightwave Technol.* **14** 58–65
[26] Kashyap R, Wyatt R and McKee P F 1993 Wavelength flattened saturated erbium amplifier using multiple side-tap Bragg gratings *Electron. Lett.* **29** 1025
[27] Peng X, Kim K, Gu X, Mielke M, Jennings S, Rider A, Fisher N, Woodbridge T, Dionne R and Trepanier F 2013 Root cause analysis and solution to the degradation of wavelength division multiplexing (WDM) couplers in high power fiber amplifier system *Opt. Express* **21** 20052–61
[28] Zhang L, Liu C, Jiang H, Qi Y, He B, Zhou J, Gu X and Feng Y 2014 Kilowatt ytterbium–Raman fiber laser *Opt. Express* **22** 18483–9
[29] Rini M, Cristiani I and Degiorgio V 2000 Numerical modeling and optimization of cascaded CW Raman fiber lasers *IEEE J. Quantum Electron.* **36** 1117–22
[30] Yablon A D 2005 *Optical Fiber Fusion Splicing* (Heidelberg: Springer)
[31] Arbore M, Zhou Y, Keaton G and Kane T 2002 36 dB gain in S-band EDFA with distributed ASE suppression *OAA* paper PD4
[32] Kim J, Dupriez P, Codemard C, Nilsson J and Sahu J K 2006 Suppression of stimulated Raman scattering in a high power Yb-doped fiber amplifier using a W-type core with fundamental mode cut-off *Opt. Express* **14** 5103–13
[33] Nicholson J W, Abeeluck A K, Headley C, Yan M F and Jorgensen C G 2003 Pulsed and continuous-wave supercontinuum generation in highly nonlinear, dispersion-shifted fibers *Appl. Phys.* B **77** 211–8
[34] Sim S K, Lim H C, Lee L W, Chia L C, Wu R F, Cristiani I, Rini M and Degiorgio V 2004 High-power cascaded Raman fibre laser using phosphosilicate fibre *Electron. Lett.* **40** 738–9
[35] Xiong Z, Moore N, Li Z G and Lim G C 2003 10 W Raman fiber lasers at 1248 nm using phosphosilicate fibers *J. Lightwave Technol.* **21** 2377–81
[36] Karpov V I *et al* 1999 Laser-diode-pumped phosphosilicate-fiber Raman laser with an output power of 1 W at 1.48 $\mu$m *Opt. Lett.* **24** 887–9
[37] Dianov E M 2002 Advances in Raman fibers *J. Lightwave Technol.* **20** 1457
[38] Supradeepa V R, Nicholson J W, Headley C, Lee Y-W, Palsdottir B and Jakobsen D Cascaded Raman fiber laser at 1480 nm with output power of 104 W *Fiber Lasers IX Technology Systems, and Applications* Proc. of SPIE vol 8237 paper 8237–48
[39] Supradeepa V R, Nicholson J W, Headley C E, Yan M F, Palsdottir B and Jakobsen D 2013 A high efficiency architecture for cascaded Raman fiber lasers *Opt. Express* **21** 7148–55
[40] Jackson S D and Muir P H 2001 Theory and numerical simulation of nth-order cascaded Raman fiber lasers *J. Opt. Soc. Am.* B **18** 1297–306
[41] Papernyi S B, Karpov V I and Clements W R L 2002 Third-order cascaded Raman amplification *Optical Fiber Communication Conf. (OFC)* FB4-1.IEEE
[42] Papernyi S, Karpov V and Clements W 2002 Cascaded pumping system and method for producing distributed Raman amplification in optical fiber telecommunication systems *US Patent* 6, 480, 326
[43] Jeong Y, Sahu J, Payne D and Nilsson J 2004 *Opt. Express* **12** 6088–92
[44] Theeg T, Ottenhues C, Sayinc H, Neumann J and Kracht D 2016 Core-pumped single-frequency fiber amplifier with an output power of 158 W. *Opt. Lett.* **41** 9–12
[45] Zhang L, Jiang H, Cui S, Hu J and Feng Y 2014 Versatile Raman fiber laser for sodium laser guide star *Laser Photon. Rev.* **8** 889–95
[46] Zhang L, Jiang H, Cui S and Feng Y 2014 Integrated ytterbium–Raman fiber amplifier *Opt. Lett.* **39** 1933
[47] Feng Y, Zhang L and Jiang H 2015 Power scaling of Raman fiber lasers *SPIE LASE* ed L B Shaw (International Society for Optics and Photonics) p 93440U
[48] Zhang L, Liu C, Jiang H, Qi Y, He B, Zhou J, Gu X and Feng Y 2014 Kilowatt ytterbium–Raman fiber laser *Opt. Express* **22** 18483
[49] Zhang H, Tao R, Zhou P, Wang X and Xu X 2015 1.5 kW Yb–Raman combined nonlinear fiber amplifier at 1120 nm *IEEE Photon. Technol. Lett.* **27** 628–30
[50] Liu J, Tan F, Shi H and Wang P 2014 High-power operation of silica-based Raman fiber amplifier at 2147 nm *Opt. Express* **22** 28383–9
[51] Shi J, Alam S and Ibsen M 2012 Highly efficient Raman distributed feedback fibre lasers *Opt. Express* **20** 5082–91
[52] Westbrook P S, Abedin K S, Nicholson J W, Kremp T and Porque J 2011 Raman fiber distributed feedback lasers *Opt. Lett.* **36** 2895–7
[53] Babin S A, Churkin D V, Ismagulov A E, Kablukov S I and Podivilov E V 2007 Four-wave-mixing-induced turbulent spectral broadening in a long Raman fiber laser *J. Opt. Soc. Am.* B **24** 1729–38
[54] Bouteiller J-C 2003 Spectral modeling of Raman fiber lasers *IEEE Photon. Technol. Lett.* **15** 1698–700
[55] Feng Y, Huang S, Shirakawa A and Ueda K I 2004 589 nm light source based on Raman fiber laser *Japan. J. Appl. Phys.* 2 **43** L722–4
[56] Agrawal G P 2007 *Nonlinear Fiber Optics* (Academic)
[57] Feng Y, Taylor L and Calia D B 2008 Multiwatts narrow linewidth fiber Raman amplifiers *Opt. Express* **16** 10927–32
[58] Vergien C, Dajani I and Zeringue C 2010 Theoretical analysis of single-frequency Raman fiber amplifier system operating at 1178 nm *Opt. Express* **18** 26214–28
[59] Supradeepa V R 2013 Stimulated Brillouin scattering thresholds in optical fibers for lasers linewidth broadened with noise *Opt. Express* **21** 4677–87
[60] Robin C and Dajani I 2011 Acoustically segmented photonic crystal fiber for single-frequency high-power laser applications *Opt. Lett.* **36** 2641–3

[61] Dajani I, Vergien C, Robin C and Ward B 2013 Investigations of single-frequency Raman fiber amplifiers operating at 1178 nm *Opt. Express* **21** 12038–52
[62] Vergien C, Dajani I and Robin C 2012 18 W single-stage single-frequency acoustically tailored Raman fiber amplifier *Opt. Lett.* **37** 1766–8
[63] Yoshizawa N and Imai T 1993 Stimulated Brillouin scattering suppression by means of applying strain distribution to fiber with cabling *Light. Technol. J.* **11** 1518–22
[64] Boggio J M C, Marconi J D and Fragnito H L 2005 Experimental and numerical investigation of the SBS-threshold increase in an optical fiber by applying strain distributions *J. Light. Technol.* **23** 3808
[65] Dajani I, Vergien C, Ward B, Robin C, Naderi S, Flores A and Diels J-C 2013 Experimental and theoretical investigations of single-frequency Raman fiber amplifiers operating at 1178 nm *Proc. SPIE* **8604** Nonlinear Frequency Generation and Conversion: Materials, Devices, and Applications XII, 86040N
[66] Engelbrecht R, Bayer M and Schmidt L P 2003 Numerical calculation of stimulated Brillouin scattering and its suppression in Raman fiber amplifiers *Lasers and Electro-Optics Europe, 2003. CLEO/Europe. 2003 Conf. on* p 641
[67] Engelbrecht R, Mueller M and Schmauss B 2009 SBS shaping and suppression by arbitrary strain distributions realized by a fiber coiling machine *2009 IEEE/LEOS Winter Topicals Meeting Series* (IEEE) pp 248–9
[68] Leng J, Chen S, Wu W, Hou J and Xu X 2011 Analysis and simulation of single-frequency Raman fiber amplifiers *Opt. Commun.* **284** 2997–3003
[69] Zhang L, Hu J, Wang J and Feng Y 2012 Stimulated-Brillouin-scattering-suppressed high-power single-frequency polarization-maintaining Raman fiber amplifier with longitudinally varied strain for laser guide star *Opt. Lett.* **37** 4796–8
[70] Engelbrecht R 2014 Analysis of SBS gain shaping and threshold increase by arbitrary strain distributions *J. Lightwave Technol.* 1–1
[71] Jackson S D 2012 Towards high-power mid-infrared emission from a fibre laser *Nat. Photon.* **6** 423–31
[72] Fortin V, Bernier M, El-Amraoui M, Messaddeq Y and Vallee R 2013 Modeling of $As_2S_3$ Raman fiber lasers operating in the mid-infrared *IEEE Photon. J.* **5** 1502309
[73] Dianov E M, Bufetov I A, Mashinsky V M, Neustruev V B, Medvedkov O I, Shubin A V, Mel'kumov M A, Gur'yanov A N, Khopin V F and Yashkov M V 2004 Raman fibre lasers emitting at a wavelength above 2 $\mu$m *Quantum Electron.* **34** 695–7
[74] Cumberland B A, Popov S V, Taylor J R, Medvedkov O I, Vasiliev S A and Dianov E M 2007 2.1 $\mu$m continuous-wave Raman laser in $GeO_2$ fiber *Opt. Lett.* **32** 1848
[75] Rakich P T, Fink Y and Soljačić M 2008 Efficient mid-IR spectral generation via spontaneous fifth-order cascaded-Raman amplification in silica fibers *Opt. Lett.* **33** 1690
[76] Jiang H, Zhang L and Feng Y 2015 Silica-based fiber Raman laser at >2.4 $\mu$m *Opt. Lett.* **40** 3249
[77] Sorokina I T, Dvoyrin V V, Tolstik N and Sorokin E 2014 Mid-IR ultrashort pulsed fiber-based lasers *IEEE J. Sel. Top. Quantum Electron.* **20** 99–110
[78] Mermelstein M D, Bouteiller J-C, Steinvurzel P, Horn C, Feder K and Eggleton B 2001 Configurable three-wavelength Raman fiber laser for Raman amplification and dynamic gain flattening *IEEE. Photon. Technol. Lett.* **13** 1286–8
[79] Mermelstein M D, Horn C, Bouteiller J-C, Steinvurzel P, Feder K, Headley C and Eggleton B J 2002 Six wavelength Raman fiber laser for C + L-band Raman amplification *CLEO '02. Technical Digest* p 478
[80] Nilsson J, Sahu J K, Jang J N, Selvas R, Hanna D C and Grudinin A B 2002 Cladding-pumped Raman fiber amplifier *Optical Amplifiers and Their Applications (OSA)* p PD2
[81] Heebner J E, Sridharan A K, Dawson J W, Messerly M J, Pax P H, Shverdin M Y, Beach R J and Barty C P J 2010 High brightness, quantum-defect-limited conversion efficiency in cladding-pumped Raman fiber amplifiers and oscillators *Opt. Express* **18** 14705–16
[82] Ji J, Codemard C A, Sahu J K and Nilsson J 2010 Design, performance, and limitations of fibers for cladding-pumped Raman lasers *Opt. Fiber Technol.* **16** 428–41
[83] Ji J 2011 *Cladding-Pumped Raman Fibre Laser Sources* (University of Southampton)
[84] Junhua J, Codemard C A and Nilsson J 2010 Analysis of spectral bendloss filtering in a cladding-pumped W-type fiber Raman amplifier *J. Lightwave Technol.* 2179–86
[85] Jiang H, Zhang L and Feng Y 2015 Cascaded-cladding-pumped cascaded Raman fiber amplifier *Opt. Express* **23** 13947
[86] Siekiera A, Engelbrecht R, Nothofer A and Schmauss B 2011 Short 17 cm DBR Raman fiber laser with a narrow spectrum in *IEEE Photon. Technol. Lett.* **24** 107–9
[87] Siekiera A, Engelbrecht R, Nothofer A and Schmauss B 2012 Characterization of a narrowband Raman MOPA with short master oscillator *Proc. SPIE* **8237** Fiber Lasers IX: Technology, Systems, and Applications, 82371I;
[88] Vatnik D, Gorbunov O A and Churkin D V 2014 Narrow-band generation and mode correlations in a short Raman fibre laser *Laser Phys.* **24** 025103
[89] Vatnik D, Gorbunov O A and Churkin D V 2014 Nonlinear mixing and mode correlations in a short Raman fiber laser *Proc. SPIE* **9136** Nonlinear Optics and Its Applications VIII; and Quantum Optics III, 913612;
[90] Kringlebotn J T, Archambault J-L, Reekie L and Payne D N 1994 $Er^{3+}$:$Yb^{3+}$ -codoped fiber distributed-feedback laser *Opt. Lett.* **19** 2101
[91] Perlin V E and Winful H G 2001 Distributed feedback fiber Raman laser *IEEE J. Quantum Electron.* **37** 38
[92] Hu Y and Broderick N G R 2009 Improved design of a DFB Raman fibre laser *Opt. Commun.* **282** 3356
[93] Lauridsen V C, Povlsen J H and Varming P 1998 Design of DFB fibre lasers *Electron. Lett.* **34** 2028
[94] Shi J and Ibsen M 2010 Effects of phase and amplitude noise on phase-shifted DFB Raman fibre lasers *Bragg Gratings Poling and Photosensitivity* JThA30
[95] Westbrook P S, Abedin K S, Nicholson J W, Kremp T and Porque J 2011 Demonstration of a Raman fiber distributed feedback laser *CLEO* paper PDPA11
[96] Shi J, Shaif-ul A and Ibsen M 2012 Sub-watt threshold, kilohertz-linewidth Raman distributed-feedback fiber laser *Opt. Lett.* **37** 1544–6
[97] Turitsyn S K, Babin S A, El-Taher A E, Harper P, Churkin D V, Kablukov S I, Ania-Castañón J D, Karalekas V and Podivilov E V 2010 Random distributed feedback fiber laser *Nat. Photon.* **4** 231–5
[98] Couny F, Benabid F and Light P S 2007 Subwatt threshold cw Raman fiber-gas laser based on $H_2$-filled hollow-core photonic crystal fiber *Phys. Rev. Lett.* **99** 143903
[99] Couny F, Mangan B J, Sokolov A V and Benabid F 2010 High power 55 Watts CW Raman fiber-gas-laser *Conf. on Lasers and Electro-Optics 2010, OSA Technical Digest (CD)* (Optical Society of America) paper CTuM3
[100] Green J T, Sikes D E and Yavuz D D 2009 Continuous-wave high-power rotational Raman generation in molecular deuterium *Opt. Lett.* **34** 2563–5
[101] Jones A *et al* 2011 Mid-IR fiber lasers based on molecular gas-filled hollow-core photonic crystal fiber *CLEO: 2011—Laser Applications to Photonic Applications, OSA Technical Digest (CD)* (Optical Society of America) paper CThD1

[102] Zhang L, Jiang H, Yang X, Pan W and Feng Y 2016 Ultra-wide wavelength tuning of a cascaded Raman random fiber laser *Opt. Lett.* **41** 215
[103] Feng Y, Huang S H, Shirakawa A and Ueda K 2004 Multiple-color cw visible lasers by frequency sum-mixing in a cascading Raman fiber laser *Opt. Express* **12** 1843–7
[104] Ageorges N and Dainty C (ed) 1997 Laser guide star adaptive optics for astronomy *NATO Adv. Study Inst.* p 551
[105] Denman C A, Hillman P D, Moore G T, Telle J M, Preston J E, Drummond J D and Fugate R Q 2005 Realization of a 50-watt facility-class sodium guidestar pump laser *Solid State Lasers XIV Technol. Devices* **5707** 46–9
[106] Lee I 2008 *20 W and 50 W Guidestar Laser System Update for the Keck I and Gemini South Telescopes* vol 7015 ed H Norbert *et al* (SPIE) p 70150N
[107] Lu Y 2015 High-average-power narrow-line-width sum frequency generation 589 nm laser *SPIE Security + Defence* ed D H Titterton *et al* (International Society for Optics and Photonics) p 965008
[108] Wang P-Y *et al* 2014 33 W quasi-continuous-wave narrow-band sodium D 2a laser by sum-frequency generation in LBO *Chin. Phys.* **23** 094208
[109] Zhang L, Yuan Y, Liu Y, Wang J, Hu J, Lu X, Feng Y and Zhu S 2013 589 nm laser generation by frequency doubling of a single-frequency Raman fiber amplifier in PPSLT *Appl. Opt.* **52** 1636–40
[110] Taylor L, Feng Y, Calia D B and Hackenberg W 2006 Multi-watt 589 nm Na $D_2$-line generation via frequency doubling of a Raman fiber amplifier: a source for LGS-assisted AO *Proc. SPIE—Int. Soc. Opt. Eng.* **6272** 627249
[111] Georgiev D, Gapontsev V P, Dronov A G, Vyatkin M Y, Rulkov A B, Popov S V and Taylor J R 2005 Watts-level frequency doubling of a narrow line linearly polarized Raman fiber laser to 589 nm *Opt. Express* **13** 6772–6
[112] Feng Y, Taylor L R and Calia D B 2009 25 W Raman-fiber-amplifier-based 589 nm laser for laser guide star *Opt. Express* **17** 19021–6
[113] Taylor L R, Feng Y and Calia D B 2010 50 W CW visible laser source at 589 nm obtained via frequency doubling of three coherently combined narrow-band Raman fibre amplifiers *Opt. Express* **18** 8540–55
[114] Kaenders W G 2010 Diode-seeded fiber-based sodium laser guide stars ready for deployment *Adaptive Optics Systems II* vol 7736 ed B L Ellerbroek *et al* (SPIE—Int. Soc. Optical Engineering)
[115] Enderlein M 2014 Series production of next-generation guide-star lasers at TOPTICA and MPBC *SPIE Astronomical Telescopes + Instrumentation* ed E Marchetti *et al* (International Society for Optics and Photonics) p 914807
[116] First Light of New Laser at Paranal | ESO (http://eso.org/public/announcements/ann15034/)
[117] $4 Million Laser Marks Ground Zero for Adaptive Optics Science W M Keck Observatory (http://keckobservatory.org/recent/entry/4_million_laser_marks_ground_zero_for_adaptive_optics_science)
[118] Phillips W D 1998 Nobel lecture: laser cooling and trapping of neutral atoms *Rev. Mod. Phys.* **70** 721–41
[119] Luo P-L, Hu J, Feng Y, Wang L-B and Shy J-T 2015 Doppler-free intermodulated fluorescence spectroscopy of $^4$He $2^3$P–$3^{1,3}$D transitions at 588 nm with a 1 W compact laser system *Appl. Phys.* B **120** 279–84
[120] Yuan Y, Zhang L, Liu Y, Lü X, Zhao G, Feng Y and Zhu S Sodium guide star laser generation by single-pass frequency doubling in a periodically poled near-stoichiometric $LiTaO_3$ crystal *Sci. CHINA Technol. Sci.* 1–4 (n.d.)
[121] Lim E-L, Shaif-ul A and Richardson D J 2012 Optimizing the pumping configuration for the power scaling of in-band pumped erbium doped fiber amplifiers *Opt. Express* **20** 13886–95
[122] Kuhn V, Kracht D, Neumann J and Weßels P 2011 Er-doped photonic crystal fiber amplifier with 70 W of output power *Opt. Lett.* **36** 3030–2
[123] Kotov L V, Likhachev M E, Bubnov M M, Medvedkov O I, Yashkov M V, Guryanov A N, Lhermite J, Février S and Cormier E 2013 75 W 40% efficiency single-mode all-fiber erbium-doped laser cladding pumped at 976 nm *Opt. Lett.* **38** 2230–2
[124] Kotov L V, Likhachev M E, Bubnov M M, Medvedkov O I, Yashkov M V, Guryanov A N, Février S, Lhermite J and Cormier E 2014 Yb-free Er-doped all-fiber amplifier cladding-pumped at 976 nm with output power in excess of 100 W *Proc. SPIE* **8961** Fiber Lasers XI: Technology, Systems, and Applications, 89610X
[125] Zhang J, Fromzel V and Dubinskii M 2011 Resonantly cladding-pumped Yb-free Er-doped LMA fiber laser with record high power and efficiency *Opt. Express* **19** 5574–8
[126] Zhang J, Fromzel V and Dubinskii M 2012 Resonantly (in-band) cladding-pumped Yb-free Er-doped fibre laser with record efficiency *Electron. Lett.* **48** 1298–300
[127] Jebali M A, Maran J-N and LaRochelle S 2014 264 W output power at 1585 nm in Er–Yb codoped fiber laser using in-band pumping *Opt. Lett.* **39** 3974–7
[128] Supradeepa V R, Nicholson J W and Feder K 2012 Continuous wave erbium-doped fiber laser with output power of >100 W at 1550 nm in-band core-pumped by a 1480 nm Raman fiber laser *CLEO Technical Digest* paper CM2N.8
[129] Ruehl A, Kuhn V, Wandt D and Kracht D 2008 Normal dispersion erbium-doped fiber laser with pulse energies above 10 nJ *Opt. Express* **16** 3130–5
[130] Nicholson J W, Jasapara J C, Desantolo A, Monberg E and Dimarcello F 2009 Characterizing the modes of a core-pumped, large-mode area Er fiber using spatially and spectrally resolved imaging *CLEO* paper CWD4
[131] Várallyay Z and Jasapara J C 2009 Comparison of amplification in large area fibers using cladding-pump and fundamental-mode core-pump schemes *Opt. Express* **17** 17242–52
[132] Lim E-L, Shaif-ul A and Richardson D J 2012 High-energy, in-band pumped erbium doped fiber amplifiers *Opt. Express* **20** 18803–18
[133] Yilmaz T *et al* 2008 Large-mode-area Er-doped fiber chirped-pulse amplification system for high-energy sub-picosecond pulses at 1.55 $\mu$m *Proc. SPIE* 6873, Fiber Lasers V: Technology, Systems, and Applications, 68731I
[134] Peng X *et al* 2014 Monolithic fiber chirped pulse amplification system for millijoule femtosecond pulse generation at 1.55 $\mu$m *Opt. Express* **22** 2459–64
[135] Nicholson J W, Ahmad R and DeSantolo A 100 W, 10 GHz, femtosecond pulses from a very-large-mode-area Er-doped fiber amplifier *Conf. on Lasers and Electro-Optics 2016* paper SM1Q.1
[136] Ramachandran S, Fini J M, Mermelstein M, Nicholson J W, Ghalmi S and Yan M F 2008 Ultra-large effective-area, higher-order mode fibers: a new strategy for high-power lasers *Laser and Photonic Reviews* (doi:10.1002/lpor.200810016)
[137] Nicholson J W, Fini J M, DeSantolo A M, Monberg E, DiMarcello F, Fleming J, Headley C, DiGiovanni D J, Ghalmi S and Ramachandran S 2010 A higher-order-mode erbium-doped-fiber amplifier *Opt. Express* **18** 17651–7
[138] Nicholson J W, DeSantolo A, Westbrook P S, Windeler R S, Kremp T, Headley C and DiGiovanni D J 2015 Axicons for mode conversion in high peak power, higher-order mode, fiber amplifiers *Opt. Express* 33849–60

[139] Nicholson J W *et al* 2012 Scaling the effective area of higher-order-mode erbium-doped fiber amplifiers *Opt. Express* **20** 24575–84
[140] Fini J M and Ramachandran S 2007 Natural bend-distortion immunity of higher-order-mode, large-mode-area fibers *Opt. Lett.* **32** 758–750
[141] Peng X *et al* 2013 Higher-order mode fiber enables high energy chirped-pulse amplification *Opt. Express* **30** 32411–6
[142] Nicholson J W, Fini J M, DeSantolo A, Westbrook P S, Windeler R S, Kremp T, Headley C and Giovanni D J 2015 High energy pulse amplification in a higher-order mode fiber amplifier with axicon for output mode conversion *Conf. on Lasers and Electro-Optics (CLEO)* paper STu4L.4
[143] Zach A, Kaenders W, Nicholson J W, Fini J and DeSantolo A 2015 Demonstration of soliton self shifting employing $Er^{3+}$ doped VLMA- and HOM-fiber amplifiers *Conf. on Lasers and Electro-Optics (CLEO)* paper ATu2M.6
[144] Jin X, Wang X, Zhou P, Xiao H and Liu Z 2015 Powerful 2 $\mu$m silica fiber sources: a review of recent progress and prospects *J. Electron. Sci. Technol.* **13** 315–27
[145] Wang X, Zhou P, Zhnag H, Wang X, Xiao H and Liu Z 2014 100 W-level Tm-doped fiber laser pumped by 1173 nm Raman fiber lasers *Opt. Lett.* **39** 4329–32
[146] Wang X, Zhou P, Miao Y, Zhang H, Xiao H, Wang X and Liu Z 2014 Raman fiber laser-pumped high-power, efficient Ho-doped fiber laser *J. Opt. Soc. Am.* B **31** 2476–9
[147] Crawford S, Hudson D D and Jackson S D 2013 High power, broadly tunable 3 $\mu$m fiber laser for the measurement of optical fiber loss *Photon. J.* 2015 **7** 1502309
[148] Zhu G, Zhu X, Balakrishnan K, Norwood R A and Peyghambarian N 2013 $Fe^{2+}$:ZnSe and graphene Q-switched singly $Ho^{3+}$-doped ZBLAN fiber lasers at 3 $\mu$m *Opt. Mater. Express* **3** 1365–77
[149] Hansen P B, Eskildsen L, Grubb S G, Stentz A J, Strasser T A, Judkins J, DeMarco J J, Pedrazzani R and DiGiovanni D J 1997 Capacity upgrades of transmission systems by Raman amplification *IEEE Photon. Technol. Lett.* **9** 262–4
[150] Masuda H, Kawai S, Suzuki K and Aida K 1997 75-nm 3-dB gain-band optical amplification with erbium-doped fluoride fiber amplifiers and distributed Raman amplifiers in 9 2 2.5 Gb/s WDM transmission *in Proc. Eur. Conf. Optical Communication* **5** 73–6
[151] Nissov M, Davidson C R, Rottwitt K, Menges R, Corbett P C, Innis D and Bergano N S 1997 100 Gb/s (10 2 10 Gb/s) WDM transmission over 7200 km using distributed Raman amplification *Proc. Eur. Conf. Optical Communication* vol 5, pp 9–12
[152] Hansen P B, Jacobovitz-Veselka G, Grüner-Nielsen L and Stentz A J 1998 Raman amplification for loss compensation in dispersion compensating fiber modules *Electron. Lett.* **34** 1136–7
[153] Lewis S A E, Chernikov S V and Taylor J R 2000 Broadband high-gain dispersion compensating Raman amplifier *Electron. Lett.* **36** 1–2
[154] Grüner-Nielsen L, Wandel M, Kristensen P, Jorgensen C, Jorgensen L V, Edvold B, Pálsdóttir B and Jakobsen D 2005 Dispersion-compensating fibers *J. Lightwave Technol.* **23** 3566
[155] Namiki S and Emori Y 2001 Ultrabroad-band Raman amplifiers pumped and gain-equalized by wavelength-division-multiplexed high-power laser diodes *IEEE J. Sel. Top. Quantum Electron.* **7** 3–16
[156] Kidorf H, Rottwitt K, Nissov M, Ma M and Rabarijaona E 1999 Pump interactions in a 100 nm bandwidth Raman amplifier *IEEE Photon. Technol. Lett.* **11** 530–2
[157] Mollenauer L F, Grant A R and Mamyshev P V 2002 Time-division multiplexing of pump wavelengths to achieve ultrabroadband, flat, backward-pumped Raman gain *Opt. Lett.* **27** 592–4
[158] Winzer P J, Sherman K and Zirngibl M 2002 Time-division multiplexed Raman pump experiment using a tunable C-band laser *IEEE Photon. Technol. Lett.* **14** 789–91
[159] Fludger C R S, Handerek V, Jolley N and Mears R J 2002 Ultra-broadband high performance distributed Raman amplifier employing pump modulation *Optical Fiber Communication Conf. and Exhibit* 2002 OFC pp 183–4
[160] Bouteiller J-C, Brar K, Bromage J, Radic S and Headley C 2003 Dual-order Raman pump *IEEE Photon. Technol. Lett.* **15** 212–4
[161] Popov S and Vanin E 2001 Polarization dependence of Raman gain on propagation direction of pump and probe signal in optical fibers *Lasers and Electro-Optics* 2001. CLEO'01. Technical Digest, pp 146–7
[162] Islam M 2004 Raman amplifiers for telecommunications 1: physical principles *Springer Series in Optical Sciences* vol 90/1
[163] Dudley J M, Genty G and Coen S 2006 Supercontinuum generation in photonic crystal fiber *Rev. Mod. Phys.* **78** 1135–84
[164] Dudley J M and Taylor J R 2010 *Supercontinuum Generation in Optical Fibers* (Cambridge University Press)
[165] Cumberland B A, Travers J C, Popov S V and Taylor J R 2008 29 W High power CW supercontinuum source *Opt. Express* **16** 5954–62
[166] Hirano M, Nakanishi T, Okuno T and Onishi M 2009 Silica-based highly nonlinear fiber and their application *IEEE J. Sel. Top. Quantum Electron.* **15** 103–13
[167] Abeeluck A K, Headley C and Jørgensen C G 2004 High-power supercontinuum generation in highly nonlinear, dispersion-shifted fibers by use of a continuous-wave Raman fiber laser *Opt. Lett.* **29** 2163–5
[168] Abeeluck A K and Headley C 2005 Continuous-wave pumping in the anomalous- and normal-dispersion regimes of nonlinear fibers for supercontinuum generation *Opt. Lett.* **30** 61–3
[169] El-Taher A E, Ania-Castañón J D, Karalekas V and Harper P 2009 High efficiency supercontinuum generation using ultra-long Raman fiber cavities *Opt. Express* **17** 17909–15
[170] Baac H W, Uribe-Patarroyo N and Bouma B E 2014 High-energy pulsed Raman fiber laser for biological tissue coagulation *Opt. Express* **22** 7113–23